2 TESTWORK

Reduction disintegrations test were conducted on a samples of Northern Cape STD, as well as several ore types from the Northern Cape deposit.

The chemical analysis of the samples before and after testing was used to determine the degree of reduction obtained during testing. The chemical analysis of the samples before testing is given in **Table 5**.

Table 5: Chemical analysis of samples before testing.

	Northern Cape STD[††]	Northern Cape OT[‡‡] 1	Northern Cape OT 2	Northern Cape OT 3	Northern Cape OT 4	Northern Cape OT 5	Northern Cape OT 6	Northern Cape OT 7
Fe (tot)	65.2	67.6	67.7	65.8	66.9	66.5	64.9	65.6
Fe2O3	92.3	96.3	96.7	93.9	95.1	94.3	92.1	93.6
FeO	0.76	0.23	0.11	0.16	0.47	0.68	0.55	0.12
Fe°	0.05	0.02	0.02	0.04	0.06	0.06	0.06	0.07
CaO	0.055	0.250	0.036	0.094	0.167	0.028	0.077	0.200
MgO	0.018	0.060	0.022	0.025	0.017	0.016	0.025	0.070
SiO2	4.06	1.73	1.96	3.92	1.60	2.86	3.51	3.66
Al2O3	1.20	0.65	0.31	0.85	1.33	1.01	2.22	1.26
K2O	0.149	0.050	0.027	0.161	0.173	0.018	0.162	0.033
Na2O	0.011	0.010	0.019	0.020	0.020	0.010	0.008	0.010
TiO2	0.062	-	0.021	0.073	0.049	0.054	0.105	0.044
MnO	0.016	0.030	0.007	0.050	0.013	0.011	0.014	0.016
P	0.048	0.037	0.036	0.028	0.068	0.040	0.044	0.035
S	0.006	0.015	0.033	0.006	0.007	0.008	0.009	0.015
C	0.035	0.023	0.022	0.028	0.036	0.042	0.046	0.038

[††] Northern Cape STD – the standard commercial mixture of natural hematite from the northern Cape region
[‡‡] OT - Ore Type

All the ore types have a good grade above 63% Fe. Of the various Northern Cape ore types OT 6 contains the lowest iron values at 64.9%. From **Table 5** it can also be seen that this ore has the highest Al_2O_3 content at 2.2%, followed by Northern Cape OT 4

The highest phosphorus is associated with the Northern Cape OT 4 lump ore at 0.068%, followed by the Northern Cape Lump STD ore, while Northern Cape OT 5 contains a maximum of 0.045% P.

Regarding K_2O levels in the lumpy ore the Northern Cape OT 6 contains the highest amounts at 0.162%, followed by the Northern Cape Lump STD ore.

2.1 REDUCTION DISINTEGRATION

To examine possible micro-structural effects, Northern Cape STD (mixed ore) and seven individual ore types from Northern Cape were tested to determine the relative reduction disintegration properties. Tests were also conducted to determine the effect of time, temperature, gas composition and size fractions on the reduction disintegration properties of the various samples.

Different standards are available to measure the low temperature reduction disintegration of ore, sinter and pellets. The method described in ISO 4696 (**Appendix 2**) was used as a basis for the test[xxvii]. During the standard test a 500g sample of –12.5+10mm material is heated under inert atmosphere (N_2) to 500°C. When the sample reaches 500°C the sample is reduced for one hour with a reducing mixture, consisting of 20% CO, 20% CO_2 and 60% N_2. The sample is then cooled down to room temperature under an inert atmosphere. A drum test and sieve analysis determines the breakdown of the sample. Results of the standard RDI test (ISO 4696) are given in **Table 6**. Because degree of reduction, gas composition and temperature were identified as factors which can influence reduction disintegration, this work included changes to the test method to determine the effect of time, temperature, size fraction and gas composition on the reduction disintegration of the various ores and ore types. The different tests are listed in

Table 7. Tests were completed in duplicate and the standard deviation was within the guidelines of the ISO standard. Similar tests on the Northern Cape samples were also conducted by SGA and the standard deviation between the two laboratories were also within the guidelines.

The furnace temperature, heating cycle and gas mixture were computer controlled to ensure repeatability of the tests. The gas flow was controlled with mass flow meters and spot checks were executed on a regular basis by means of a mass spectrometer. The temperatures were controlled within ±10°C of the desired temperature. The tests were conducted in duplicate according to the specifications in ISO 4696 and the average of the test results is reported.

Table 6: RDI results of samples according to ISO 4696

Sample	ISO 4696		
	$RDI_{+6.3mm}$	$RDI_{+3.15mm}$	$RDI_{-0.5mm}$
Northern Cape STD	90.86	94.10	1.93
NORTHERN CAPE OT 1	90.00	93.90	2.10
Northern Cape OT 2	76.90	84.96	6.15
Northern Cape OT 3	87.20	93.40	1.70
Northern Cape OT 4	98.92	99.34	0.30
Northern Cape OT 5	89.92	93.96	1.77
Northern Cape OT 6	79.57	87.35	3.59
Northern Cape OT 7	90.80	95.10	1.80

Table 7: List of different tests performed.

Test nr	Ore Type	Size fraction	Changes made to ISO 4696
1	Northern Cape STD	-25+20mm	Size Fraction
2	Northern Cape STD	-20+16mm	Size Fraction
3	Northern Cape STD	-16+12.5mm	Size Fraction
4	Northern Cape STD	-12.5+10mm	No Change
5	Northern Cape STD	-10+8mm	Size Fraction
6	Northern Cape OT 1	-12.5+10mm	No Change
7	Northern Cape OT 2	-12.5+10mm	No Change
8	Northern Cape OT 3	-12.5+10mm	No Change
9	Northern Cape OT 4	-12.5+10mm	No Change
10	Northern Cape OT 5	-12.5+10mm	No Change
11	Northern Cape OT 6	-12.5+10mm	No Change
12	Northern Cape OT 7	-12.5+10mm	No Change
13	Northern Cape STD	-25+20mm	Size Fraction, Increase time 90 min
14	Northern Cape STD	-20+16mm	Size Fraction, Increase time 90 min
15	Northern Cape STD	-16+12.5mm	Size Fraction, Increase time 90 min
16	Northern Cape STD	-12.5+10mm	Increase time 90 min
17	Northern Cape STD	-10+8mm	Size Fraction, Increase time 90 min
18	Northern Cape STD	-25+20mm	Size Fraction, Increase time 120 min
19	Northern Cape STD	-20+16mm	Size Fraction, Increase time 120 min
20	Northern Cape STD	-16+12.5mm	Size Fraction, Increase time 120 min
21	Northern Cape STD	-12.5+10mm	Increase time 120 min
22	Northern Cape STD	-10+8mm	Size Fraction, Increase time 120 min
23	Northern Cape STD	-12.5+10mm	Increase Temp 550°C
24	Northern Cape STD	-12.5+10mm	Increase Temp 600°C
25	Northern Cape STD	-12.5+10mm	Increase Temp 650°C
26	Northern Cape STD	-12.5+10mm	Increase Temp 700°C
27	Northern Cape STD	-12.5+10mm	Enrich gas composition 5% H_2
28	Northern Cape STD	-12.5+10mm	Enrich gas composition 10% H_2
29	Northern Cape STD	-12.5+10mm	Increase Temp 600°C, Increase time 90 min
30	Northern Cape STD	-12.5+10mm	Increase Temp 600°C, Increase time 120 min
31	Northern Cape STD	-12.5+10mm	Increase Temp 700°C, Increase time 90 min
32	Northern Cape STD	-12.5+10mm	Increase Temp 700°C, Increase time 120 min
33	Northern Cape STD	-12.5+10mm	Increase Temp 750°C, 60 min
34	Northern Cape STD	-12.5+10mm	Increase Temp 800°C, 60 min

2.2 EVALUATION OF CRACK OCCURANCE AND PROPAGATION

Samples of the different size fractions generated during the reduction disintegration tests were analyzed using a scanning electron microscope (SEM). The aim of this part of the study was to determine whether the cracks are significantly associated with specific phases, i.e. to determine whether the cracks follow ore particles, and whether they occur in the hematite matrix or the gangue portion of the ore.

Five different ore types were examined, namely:

- Northern Cape STD -10+8mm (Test 5)
- Northern Cape OT 2 (Test 7)
- Northern Cape OT 4 (Test 9)
- Northern Cape OT 5 (Test 10)
- Northern Cape OT 6 (Test 11)

2.2.1 Analysis Method

A point counting method was used to evaluate the images from the SEM analysis and only images of the same magnification (X120) were considered for analyses. A representative pool image was used for the counts.

A grid was used for the fracture distribution determination. The number of cracks that fell on the intersection was counted: it was recorded whether the crack occurred in the iron ore matrix or in gangue minerals. The same grid was used to record the percentage of gangue minerals vs hematite in the samples. The methodology is illustrated in **Figure 32**. **Table 8** is a summary of the results as presented in **Figure 32**. It should be noted that this is merely a demonstration and does not apply to any of the data discussed.

Table 8: Illustrative data using Figure 32 to illustrate the methodology used to evaluate the occurrences of cracks using SEM analysis.

	Cracks assoc. with Ore	Cracks assoc. with gangue	Gangue	Hematite
Count	1	3	16	55
Percentage	25	75	22.5	77.5

SEM analysis was carried out on all the size fractions produced during the reduction disintegration tests.

2.3 HIGH TEMPERATURE MICROSCOPE REDUCTION TESTS

High temperature microscopy was performed during reduction, to follow crack formation and crack propagation. **Figure 33** is a graphical representation of the high temperature microscope at Wollongong University, which is the instrument that was used. The sample is heated with the halogen lamp (1kW). The lamp is air cooled, with the furnace housing water-cooled. The samples were prepared to fit in a 10mm outer diameter (alumina) 8mm inner and 3mm high alumina crucible. The samples were polished to get an even surface to simplify the use of the microscope. A Lasertec microscope (Model 1LM21) was used, while the video signal was captured using a Snazzi AVIO capturecard.

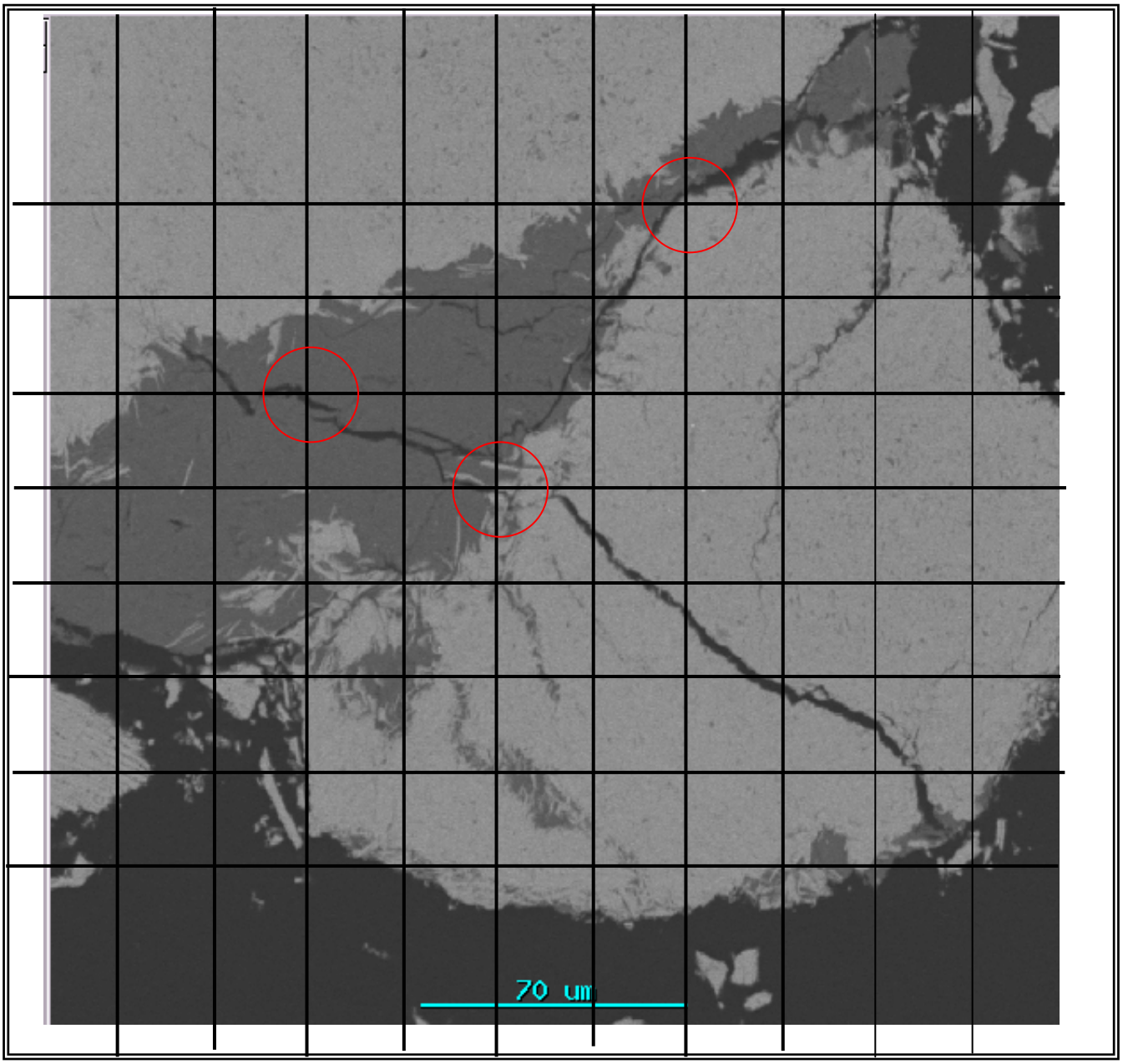

Figure 32: Illustration of methodology used to evaluate the occurrences of cracks using SEM images.

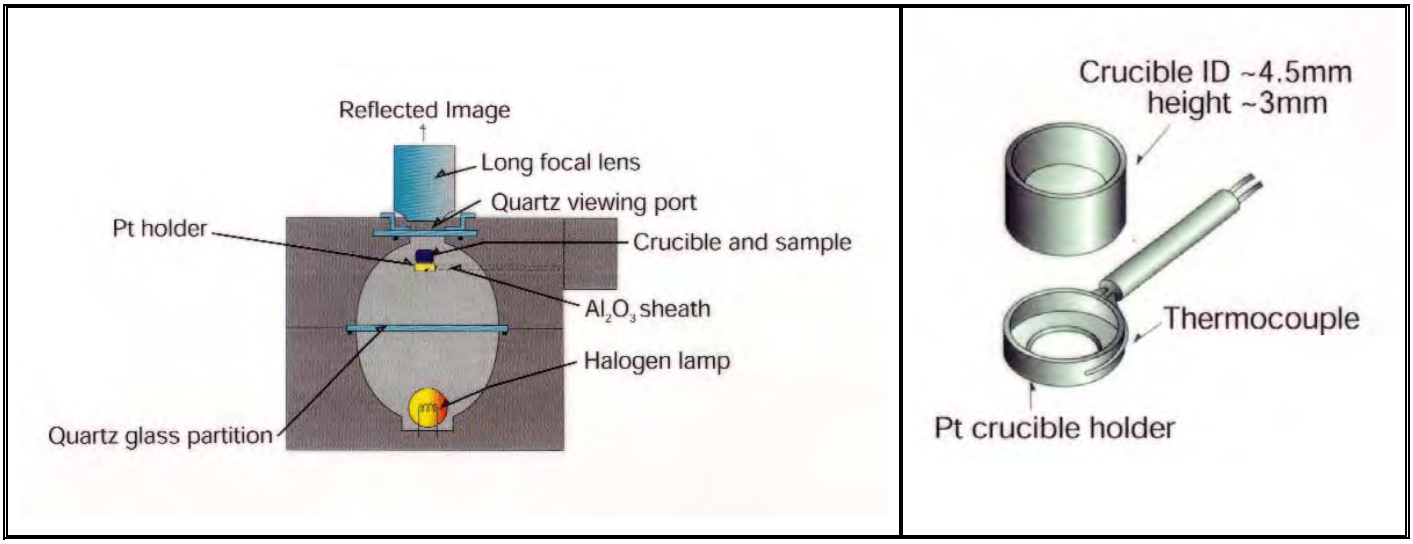

Figure 33: Graphical representation of high temperature microscope.

Table 9 lists the original sample labels as well as the reduction atmosphere under which the samples were heated. The test procedure of ISO 4696 was used as basis for the test procedure. During heating and cooling, BOC UHP (ultra high purity) Ar was passed through a Vici He purifier (used for all noble gasses) and used as inert atmosphere. A pre-mix gas from Air Liquide (20% CO, 20% CO_2 and 60% N_2) was used as a reduction gas for the CO runs. BOS Argoplas 5 (5% H_2 in Ar) was used for the hydrogen runs. A flow rate of approximately 2l/min was used.

Due to non-uniform heating of the sample (under inert conditions), the heating rate was decreased so that the samples were heated from 0-500ºC in one hour. **Figure 34** is an illustration of the test conditions used in the high temperature microscope. During the tests, a video recording was made of the entire test. Emphasis was placed on crack formation and propagation. A magnification of 10 times (objective) was used.

After the reduction test, the samples were mounted in epoxy resin, polished and coated with gold in a sputter coater. They were observed in a JOEL 5800 scanning electron microscope at the Department of Microscopy and Micro-Analysis at the University of Pretoria.

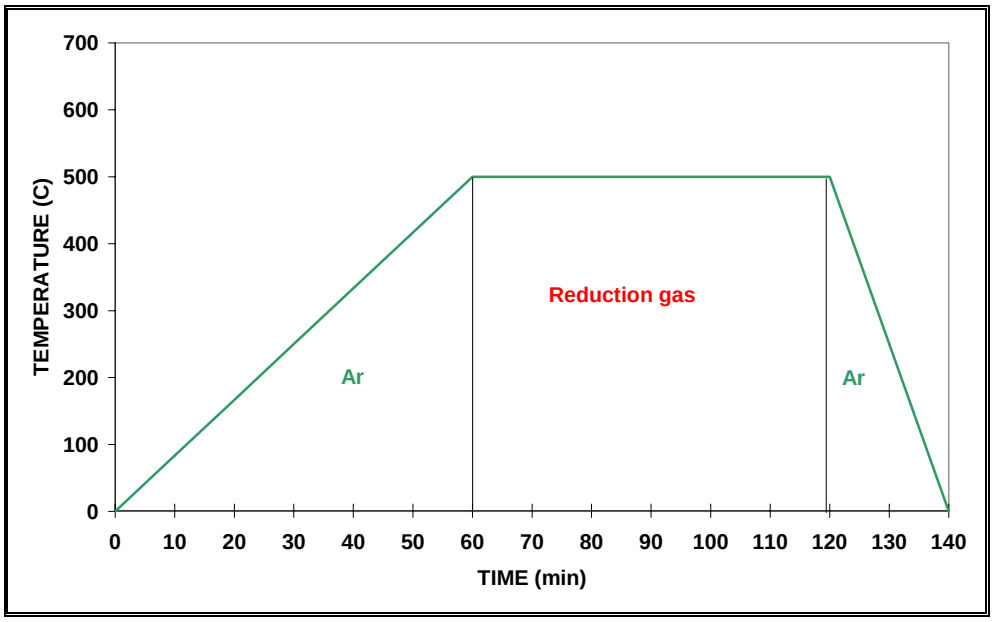

Figure 34: Illustration of test conditions used in the high temperature microscope.

Table 9: List and test conditions of samples reduced under the high temperature microscope.

Sample No.	Sample Name	Date	Reduction gas composition (%) Remaining = Ar	Time (min) and reduction temp (ºC)
1	Northern Cape OT 5	13/06/06	20 CO, 20 CO_2	60; 500
2	Northern Cape OT 2	14/06/06	20 CO, 20 CO_2	60; 500
3	Northern Cape OT 4	09/06/06	20 CO, 20 CO_2	60; 500
6	Northern Cape OT 2	13/06/06	20 CO, 20 CO_2	60; 500
8	Northern Cape STD	09/06/06	20 CO, 20 CO_2	60; 500
10	Northern Cape OT 4	09/06/06	20 CO, 20 CO_2	60; 500
12	Northern Cape OT 2	14/06/06	20 CO, 20 CO_2	60; 500
13	Northern Cape STD	12/06/06	20 CO, 20 CO_2	60; 500
14	Northern Cape OT 6	13/06/06	20 CO, 20 CO_2	60; 500
15	Northern Cape OT 6	14/06/06	20 CO, 20 CO_2	60; 500
16	Northern Cape STD	12/06/06	20 CO, 20 CO_2	60; 500
17	Northern Cape OT 4	12/06/06	20 CO, 20 CO_2	60; 500
18	Northern Cape STD	27/02/07	5 H_2	120; 500
19	Northern Cape STD	1/3/2003	5 H_2	180; 500
20	Northern Cape STD	7/3/2007	5 H_2	180; 500
21	Northern Cape STD	9/3/2003	20 CO, 20 CO_2	90; 700

3 RESULTS

3.1 REDUCTION DISINTEGRATION

The results of the sieve analysis and the degree of reduction after the various reduction disintegration tests are given in **Table 10**. All the results were within the prescribed repeatability procedure given in the ISO standard (ISO 4696) where the difference of the two duplicate tests should be less than 0.5. The forms of iron used to calculate the percentage reduction is given in **Table 11** for the different ore types. The variance of the chemical analysis was stated 0.12 for Fe(tot) (wet chemical) and 0.28 for FeO (ICP). It should be noted that the Fe_2O_3 value is a calculated value. **Table 12** shows the XRD-analysis for the different ore types. These results indicate that the FeO measured during the wet chemical analysis is in the form of magnetite and no wüstite was formed during reduction. More comprehensive tables are given in **Appendix 3.**

Figure 35 indicates the effect of burden size on the degree of reduction disintegration on Northern Cape STD. From the graphs it is clear that the degree of reduction disintegration is very similar despite differences in the burden size. It is only for the burden size -10+8mm that a significant increase in the percentage fine material is noted. This is mainly due to the fact that the burden material size fraction is merely +8mm, hence only a small degree of size degradation is required to produce a significant amount of -8mm material.

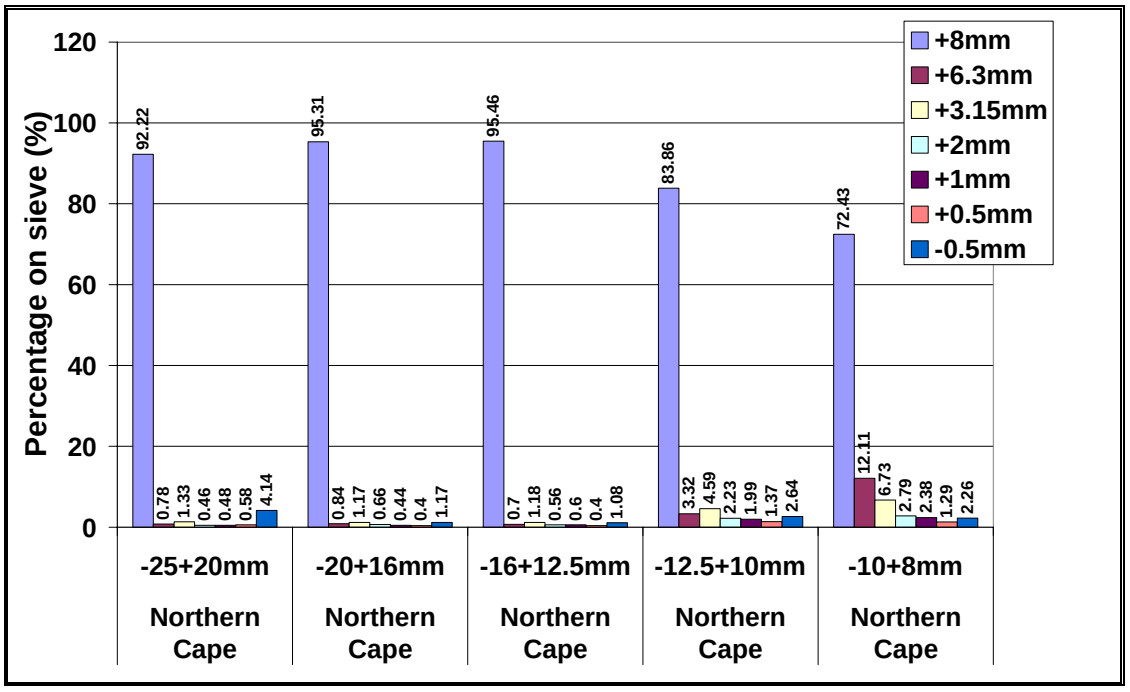

Figure 35: Effect of burden size on the degree of reduction disintegration on Northern Cape STD.

Table 10: Results of sieve analysis and fractional reduction after reduction disintegration testing

Test no.	Ore Type	Size fraction (Original)	Size fraction after RDI		% Reduction		
			+6.3mm	-6.3mm	+6.3mm	-6.3mm	Total
1	Northern Cape STD	-25+20mm	93.00	6.99	1.29	1.78	1.36
2	Northern Cape STD	-20+16mm	96.15	3.84	0.78	0.00	0.75
3	Northern Cape STD	-16+12.5mm	96.16	3.82	1.09	0.00	1.05
4	Northern Cape STD	-12.5+10mm	90.86	9.14	1.73	5.49	2.07
5	Northern Cape STD	-10+8mm	84.54	15.45	2.78	4.13	2.99
6	Northern Cape OT 1	-12.5+10mm	90.00	10.10	0.42	4.43	0.83
7	Northern Cape OT 2	-12.5+10mm	76.90	23.10	0.94	4.11	1.67
8	Northern Cape OT 3	-12.5+10mm	87.20	12.80	1.43	4.40	1.81
9	Northern Cape OT 4	-12.5+10mm	98.92	1.08	0.03	12.76	0.17
10	Northern Cape OT 5	-12.5+10mm	89.92	10.09	2.37	6.06	2.74
11	Northern Cape OT 6	-12.5+10mm	79.57	20.43	3.44	4.31	3.62

Test no.	Ore Type	Size fraction (Original)	Size fraction after RDI		% Reduction		
			+6.3mm	-6.3mm	+6.3mm	-6.3mm	Total
12	Northern Cape OT 7	-12.5+10mm	90.80	9.20	5.06	7.05	5.25
13	Northern Cape STD	-25+20mm	98.59	1.40	0.00	0.00	0.00
14	Northern Cape STD	-20+16mm	90.25	9.74	0.32	5.54	0.82
15	Northern Cape STD	-16+12.5mm	86.61	13.38	0.00	0.00	0.00
16	Northern Cape STD	-12.5+10mm	83.61	16.39	2.27	5.75	2.84
17	Northern Cape STD	-10+8mm	78.29	21.71	2.42	4.60	2.90
18	Northern Cape STD	-25+20mm	94.21	5.78	0.00	0.00	0.00
19	Northern Cape STD	-20+16mm	87.24	12.76	0.00	0.00	0.00
20	Northern Cape STD	-16+12.5mm	77.46	22.54	3.26	5.69	3.81
21	Northern Cape STD	-12.5+10mm	82.60	17.40	0.78	6.17	1.72
22	Northern Cape STD	-10+8mm	71.88	28.12	2.79	4.78	3.35
23	Northern Cape STD	-12.5+10mm	86.70	13.30	3.05	5.80	3.42
24	Northern Cape STD	-12.5+10mm	87.10	12.90	0.82	6.88	1.60
25	Northern Cape STD	-12.5+10mm	87.80	12.20	1.63	7.68	2.37
26	Northern Cape STD	-12.5+10mm	87.30	12.70	4.60	9.78	5.26
27	Northern Cape STD	-12.5+10mm	91.00	9.00	3.41	6.16	3.66
28	Northern Cape STD	-12.5+10mm	87.10	12.90	7.42	6.50	7.30
29	Northern Cape STD	-12.5+10mm	86.45	13.55	2.12	8.36	2.96
30	Northern Cape STD	-12.5+10mm	76.30	23.70	5.12	6.27	5.39
31	Northern Cape STD	-12.5+10mm	88.40	11.60	6.25	10.72	6.77
32	Northern Cape STD	-12.5+10mm	80.80	19.20	4.25	11.65	5.67
33	Northern Cape STD	-12.5+10mm	92.00	8.00	3.19	15.07	4.14
34	Northern Cape STD	-12.5+10mm	94.70	5.30	4.63	15.09	5.19

Table 11: Chemical analysis of the different size fractions after reduction disintegration tests for the different ore types.

Sample Name/ Test no.	Ref No.	Size Fraction	Fe_{total}	Fe^{o}	FeO	Fe_2O_3
Northern Cape STD/Test no 4	RMT 2540	+8mm	66.65	0.07	5.40	89.20
	RMT 2541	+6.3mm	68.08	0.18	9.21	86.86
	RMT 2542	+3.15mm	68.96	0.04	14.17	82.80
	RMT 2543	+1mm	70.01	3.46	23.55	68.98
	RMT 2544	-0.5mm	68.62	Insufficient Sample		98.13
Northern Cape OT 1/ Test no 6	RMT 2545	+10mm	68.29	0.14	3.17	93.93
	RMT 2546	+8mm	68.29	0.13	4.74	92.20
	RMT 2547	+6.3mm	70.16	0.20	8.83	90.22

	RMT 2548	+3.15mm	69.81	0.07	14.95	83.10
	RMT 2549	+2mm	70.85	0.55	22.74	75.24
	RMT 2550	+1mm	70.98	0.21	25.29	73.08
	RMT 2551	+0.5mm	70.38	Insufficient Sample		100.64
	RMT 2552	-0.5mm	68.99	0.24	24.49	71.08
Northern Cape OT 2/ Test no 7	RMT 2553	+10mm	68.85	0.12	6.28	91.30
	RMT 2554	+8mm	69.24	0.13	7.24	90.78
	RMT 2555	+6.3mm	68.65	0.09	9.70	87.25
	RMT 2556	+3.15mm	70.42	0.18	12.25	86.82
	RMT 2557	+2mm	70.22	0.16	18.46	79.66
	RMT 2558	+1mm	70.88	0.03	24.87	73.66
	RMT 2559	+0.5mm	70.41	0.53	24.22	73.00
	RMT 2560	-0.5mm	69.39	0.09	25.75	70.47
Northern Cape OT 3/ Test no 8	RMT 2561	+10mm	65.93	0.03	3.48	90.37
	RMT 2562	+8mm	67.91	0.18	4.39	91.97
	RMT 2563	+6.3mm	65.05	0.05	4.07	88.42
	RMT 2564	+3.15mm	66.51	0.08	9.19	84.78
	RMT 2565	+2mm	68.19	0.34	16.93	78.20
	RMT 2566	+1mm	68.36	0.20	21.47	73.59
	RMT 2567	+0.5mm	67.82	0.11	22.40	71.92
	RMT 2568	-0.5mm	65.02	0.46	21.64	68.26
Northern Cape OT 4/ Test no 9	RMT 2569	+10mm	67.16	0.20	1.80	93.75
	RMT 2570	+8mm	65.75	0.17	1.93	91.63
Northern Cape OT 5/ Test no 10	RMT 2571	+10mm	66.74	0.13	4.61	90.13
	RMT 2572	+8mm	67.39	0.18	5.88	89.57
	RMT 2573	+6.3mm	68.28	0.12	10.10	86.24
	RMT 2574	+3.15mm	68.24	0.04	12.31	83.84
	RMT 2575	+2mm	67.88	0.41	17.51	77.01
	RMT 2576	+1mm	67.85	Insufficient Sample		97.03
	RMT 2577	+0.5mm	68.54	0.08	21.76	73.70
	RMT 2578	-0.5mm	66.20	0.13	22.59	69.36
Northern Cape OT 6/ Test no 11	RMT 2611	+10mm	64.81	0.10	3.81	88.30
	RMT 2612	+8mm	66.26	0.15	5.49	88.43
	RMT 2613	+6.3mm	68.67	0.22	8.21	88.75
	RMT 2614	+3.15mm	68.20	0.13	12.36	83.60
	RMT 2615	+2mm	68.40	Insufficient Sample		97.81
	RMT 2616	+1mm	69.61	0.04	23.15	73.74
	RMT 2617	+0.5mm	68.42	Insufficient Sample		97.84
	RMT 2618	-0.5mm	66.36	0.19	23.04	69.00
Northern Cape OT 7/ Test no 12	RMT 3197	+10mm	65.00	0.01	5.11	87.20
	RMT 3198	+8mm	65.90	0.01	6.00	87.60
	RMT 3199	+6.3mm	64.00	0.07	7.21	83.40
	RMT 3200	+3.15mm	66.80	0.03	10.10	84.20
	RMT 3201	+2mm	66.30	0.03	15.70	77.30
	RMT 3202	+1mm	67.40	0.19	20.80	73.00
	RMT 3203	+0.5mm	67.60	0.20	25.00	68.60
	RMT 3204	-0.5mm	65.80	0.19	23.90	67.20

Table 12: XRD analysis of the different size fractions after reduction disintegration tests for the different ore types.

Sample Name/ Test no.	Ref No.	Size Fraction	% Hematite	% Magnetite	% Quartz	% Calcite	% Clay
Northern Cape STD/Test no 4	RMT 2540	+8mm	78.6	13.5	7.9	-	-
	RMT 2541	+6.3mm	72.7	24.9	2.4	-	-
	RMT 2542	+3.15mm	60	35	5	-	-
	RMT 2543	+1mm	18.5	73.3	8.2	-	-
	RMT 2544	-0.5mm	14.6	68.4	16.9	-	-
Northern Cape OT 1/ Test no 6	RMT 2545	+10mm	82.7	11.4	3.2	-	2.8
	RMT 2546	+8mm	85.3	10.3	4.5	-	-
	RMT 2547	+6.3mm	75	22.4	2.5	-	-
	RMT 2548	+3.15mm	61.2	36.5	2.3	-	-
	RMT 2549	+2mm	30.6	66	3.4	-	-
	RMT 2550	+1mm	17.4	79.8	2.8	-	-
	RMT 2551	+0.5mm	10.6	83.8	5.5	-	-
	RMT 2552	-0.5mm	7.7	81.3	11	-	-
Northern Cape OT 2/ Test no 7	RMT 2553	+10mm	84.4	12.4	3.2	-	-
	RMT 2554	+8mm	81.6	15.5	2.9	-	-
	RMT 2555	+6.3mm	76.3	19.9	3.8	-	-
	RMT 2556	+3.15mm	75.8	22.7	1.4	-	-
	RMT 2557	+2mm	44.6	50.9	4.5	-	-
	RMT 2558	+1mm	23.3	72.8	3.9	-	-
	RMT 2559	+0.5mm	12.5	82	5.4	-	-
	RMT 2560	-0.5mm	9.4	82.2	8.4	-	-
Northern Cape OT 3/ Test no 8	RMT 2561	+10mm	83.3	8.8	8	-	-
	RMT 2562	+8mm	85.3	9.4	5.4	-	-
	RMT 2563	+6.3mm	82.3	6.4	11.3	-	-
	RMT 2564	+3.15mm	67.3	20.4	12.3	-	-
	RMT 2565	+2mm	53.8	37.4	8.9	-	-
	RMT 2566	+1mm	27.9	58.7	13.4	-	-
	RMT 2567	+0.5mm	16.9	67.3	15.8	-	-
	RMT 2568	-0.5mm	12.8	64.7	22.5	-	-
Northern Cape OT 4/ Test no 9	RMT 2569	+10mm	95.6	3.1	1.2	-	-
	RMT 2570	+8mm	94.4	0	3	-	2.6
Northern Cape OT 5/ Test no 10	RMT 2571	+10mm	83.5	10.3	6.2	-	-
	RMT 2572	+8mm	82	13.4	4.6	-	-
	RMT 2573	+6.3mm	78.7	19.3	2.1	-	-
	RMT 2574	+3.15mm	72.1	23.5	4.4	-	-
	RMT 2575	+2mm	53.4	38.7	7.7	-	-
	RMT 2576	+1mm	18.2	73.1	8.7	-	-
	RMT 2577	+0.5mm	36.4	57.2	6.4	-	-
	RMT 2578	-0.5mm	11	78.6	10.4	-	-
Northern Cape OT 6/ Test no 11	RMT 2611	+10mm	86.9	6.6	2.1	-	4.5
	RMT 2612	+8mm	87	10	3	-	-
	RMT 2613	+6.3mm	83.3	13.7	3	-	-
	RMT 2614	+3.15mm	67.9	24.6	4.5	-	3
	RMT 2615	+2mm	47	48.7	4.3	-	-
	RMT 2616	+1mm	22.8	73.8	3.4	-	-
	RMT 2617	+0.5mm	13.6	79.2	7.2	-	-
	RMT 2618	-0.5mm	7.1	80.5	8.2	-	4.1

Figure 36 indicates the effect of ore composition and microstructure on the degree of reduction disintegration. The results indicate that Northern Cape OT 4 is very stable with 98 percent of the material greater than 8mm. This correlates with the low degree of reduction that was recorded for this ore type. In contrast, Northern Cape OT 7, that performed second best with regards to the degree of reduction disintegration, recorded the highest average degree of reduction of 5.2%. On the other hand for Northern Cape OT 2 and Northern Cape OT 6 only 70-75 percent of the material is greater than 8mm. Although the general thinking is that the disintegration is mainly due to the reduction process, the average degree of reduction for Northern Cape OT 2 is 1.7 percent while that of Northern Cape OT 6 is 3.8 percent (**Figure 37**).

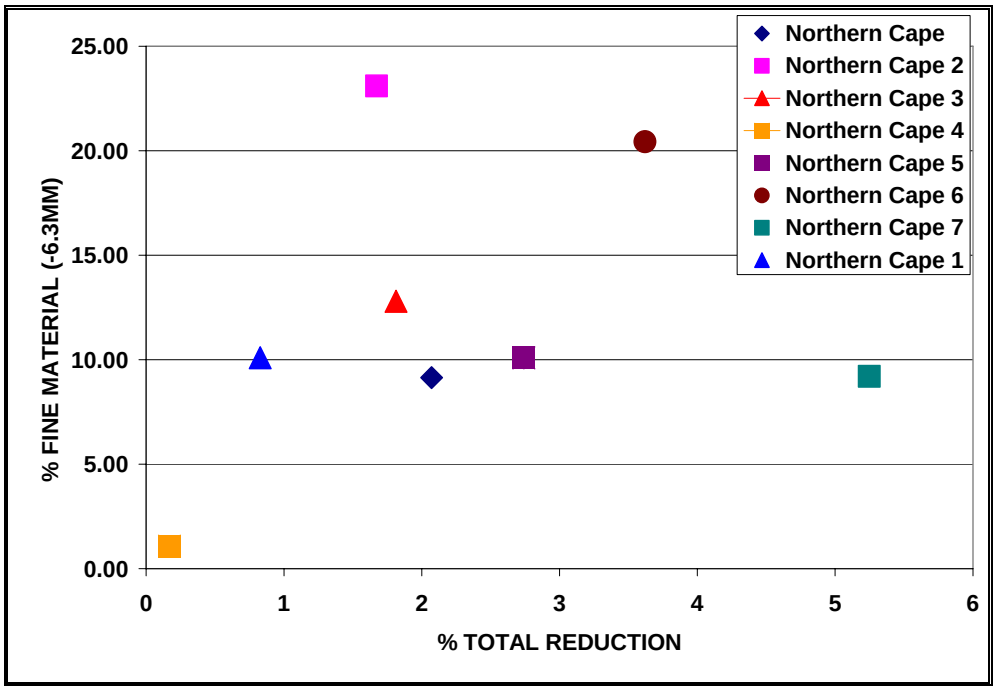

Figure 37 These results suggest that the degree of breakdown depends both on the reduction process as well as the microstructure of the ore.

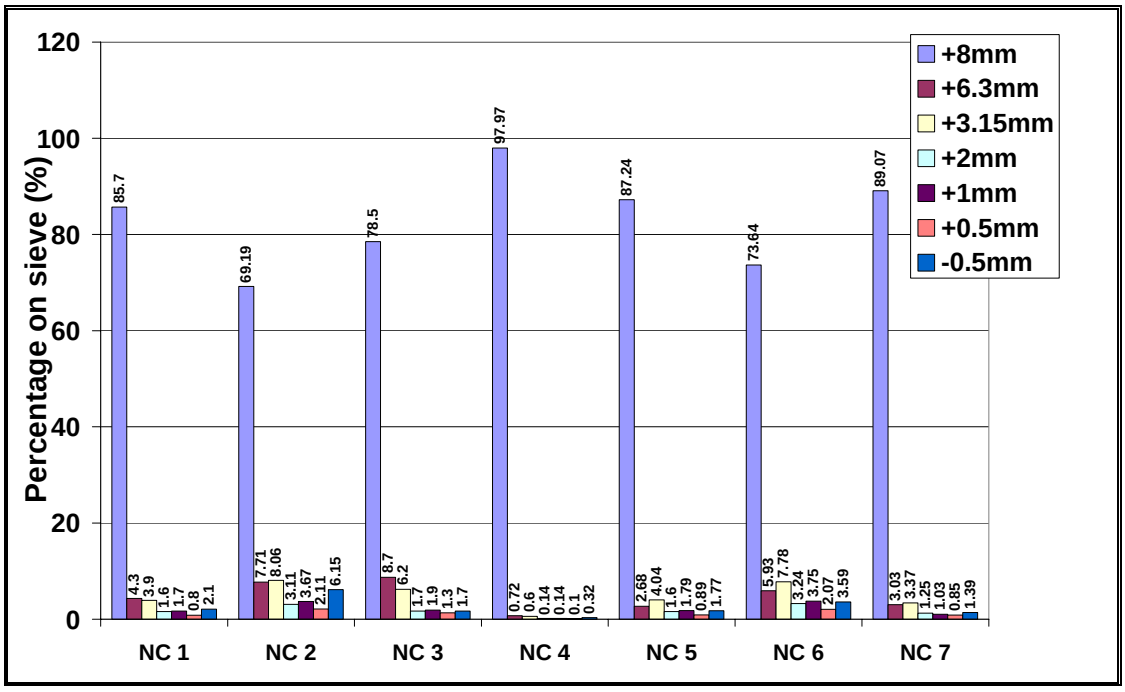

Figure 36: Degree of reduction disintegration for the different Northern Cape Ore types.

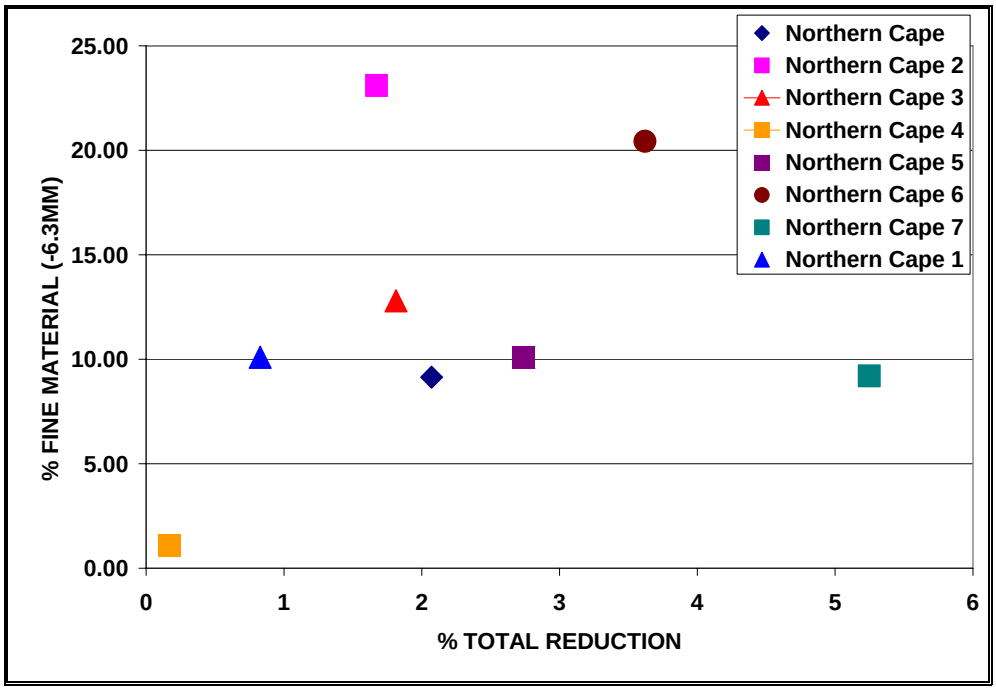

Figure 37: Percentage reduction after reduction disintegration tests for Northern Cape STD and the various ore types plotted against the % fine material (-6.3mm) generated during the test.

The effect of H_2 on the degree of reduction and the percentage fine material generated is indicated in **Figure 38**. In the first test where 5% H_2 is added to the reduction mix, the percentage reduction nearly doubled, without increasing the % fines generated. Doubling the amount of H_2 in the reduction mixture again doubles the percentage reduction, but the percentage fines generated only increases with about 40%.

Figure 39 is a graphical representation of the effect of reduction time on reduction disintegration for samples of different sizes tested for Northern Cape STD. For the -25+20mm burden, an increase in reduction time apparently leads to a decrease in the degree of reduction disintegration (this effect is likely to be reflect test-to-test variation rather than any fundamental effect). The -20+16mm burden material indicated a slight increase in the percentage +16mm, but there is also an increase in the percentage finer material that forms with an increase in time from 60 minute to 90 minutes. Increasing the reduction time further to 120 minutes leads to a general increase in the degree of reduction disintegration.

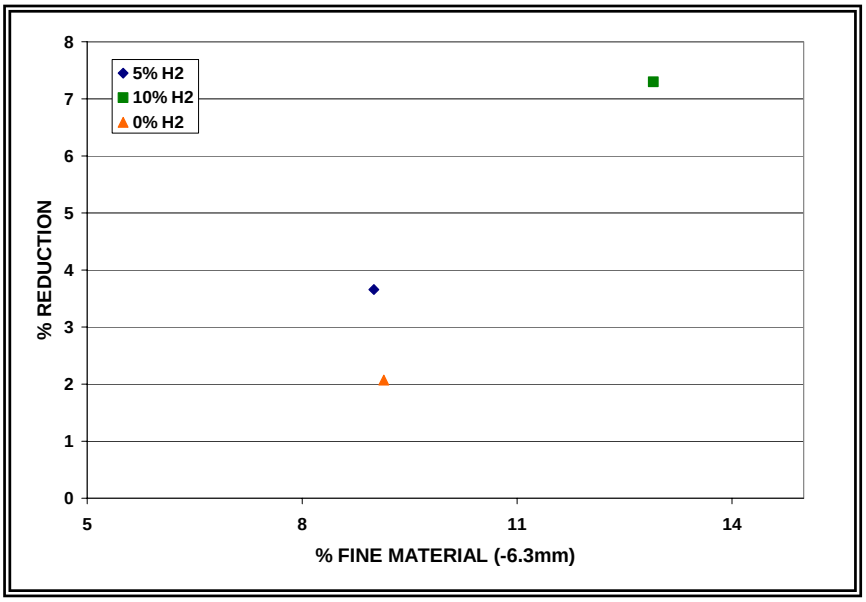

Figure 38: Effect of gas composition on the degree of reduction and the percentage fine material generated.

For the -16+12.5mm, -12.5+10mm and -10+8mm starting materials, a general trend was noted of an increase in the degree of reduction disintegration with an increase in reduction time. To determine whether the same tendency is valid at higher temperatures, tests were also conducted at 600°C and 700°C with the -12.5+10mm burden. The results of these tests are indicated in **Figure 40**. This graph confirms that an increase in reduction time leads to a general increase in the degree of reduction disintegration, independent of the reduction temperature.

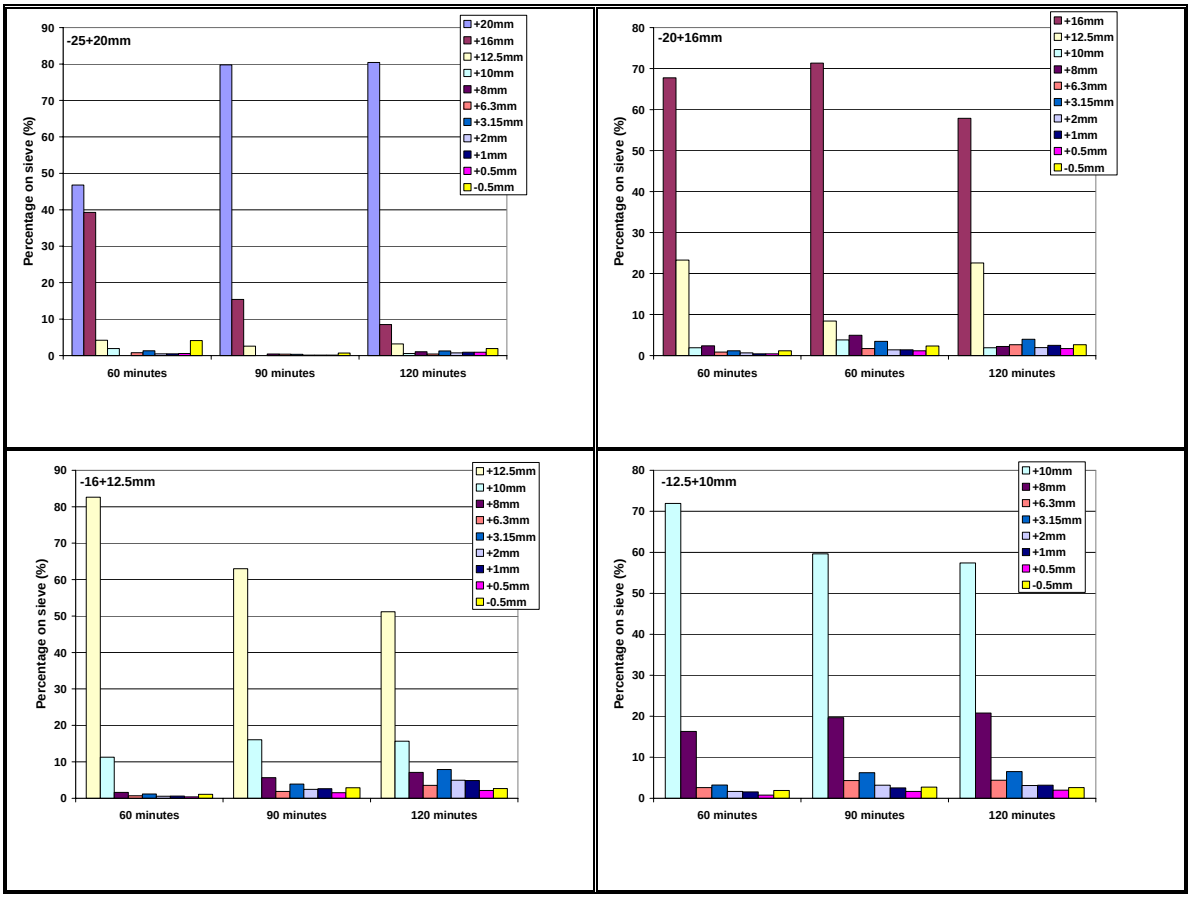

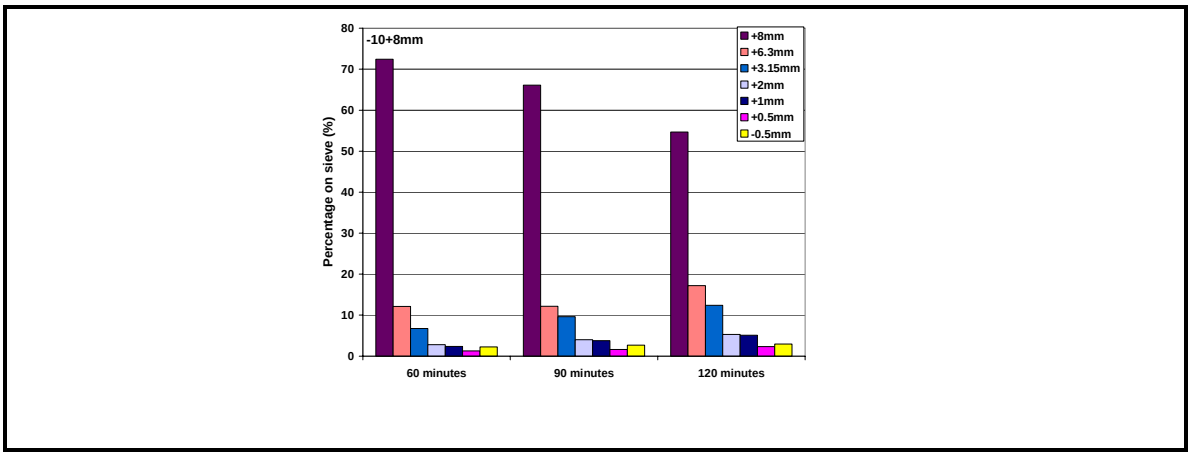

Figure 39: Effect of reduction time on the degree of reduction disintegration for samples of different sizes of Northern Cape STD.

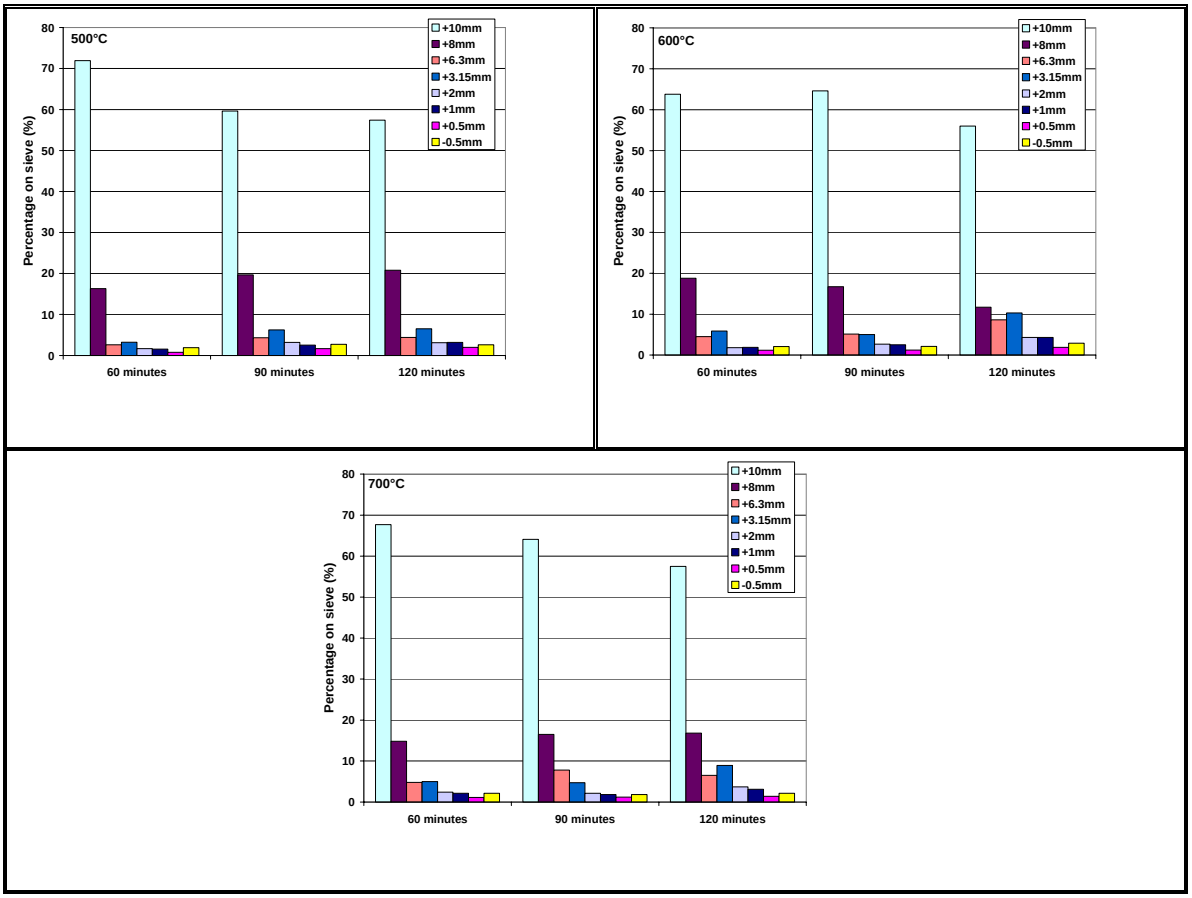

Figure 40: Effect of temperature on reduction disintegration for -12.5+10mm burdens after 60, 90 and 120 minutes of Northern Cape STD.

Figure 41 indicates the effect of reduction time and temperature on the percentage fines generated. This graph shows a general upward trend in the percentage fine generated for increasing temperatures and increasing reduction times.

Figure 42 indicates the effect of reduction temperature on the degree of reduction disintegration on a -12.5+10mm fraction burden for Northern Cape STD. The figure confirms that between 500°C and 700°C similar degrees of reduction disintegration is noted, but with a decline in the degree of reduction disintegration above 700°C. **Figure 43** represents the same results as percentage fines generated compared to reduction temperature. From the figure it is clear that at temperature between 550°C and 700°C the percentage fines generated increase by 50 percent and more compared to temperatures of 500°C, 750°C and 800°C.

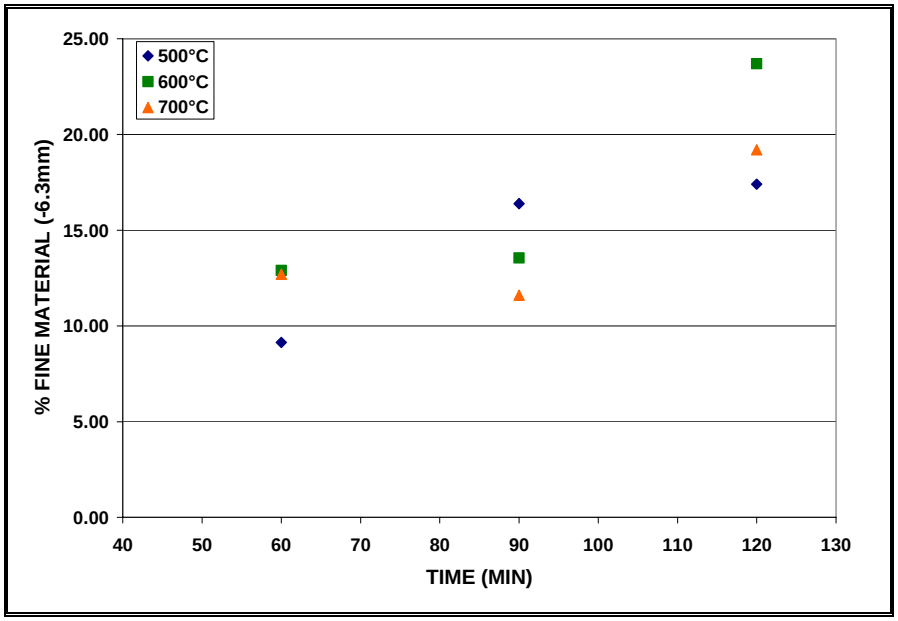

Figure 41: Effect of time and temperature on the reduction disintegration of Northern Cape STD

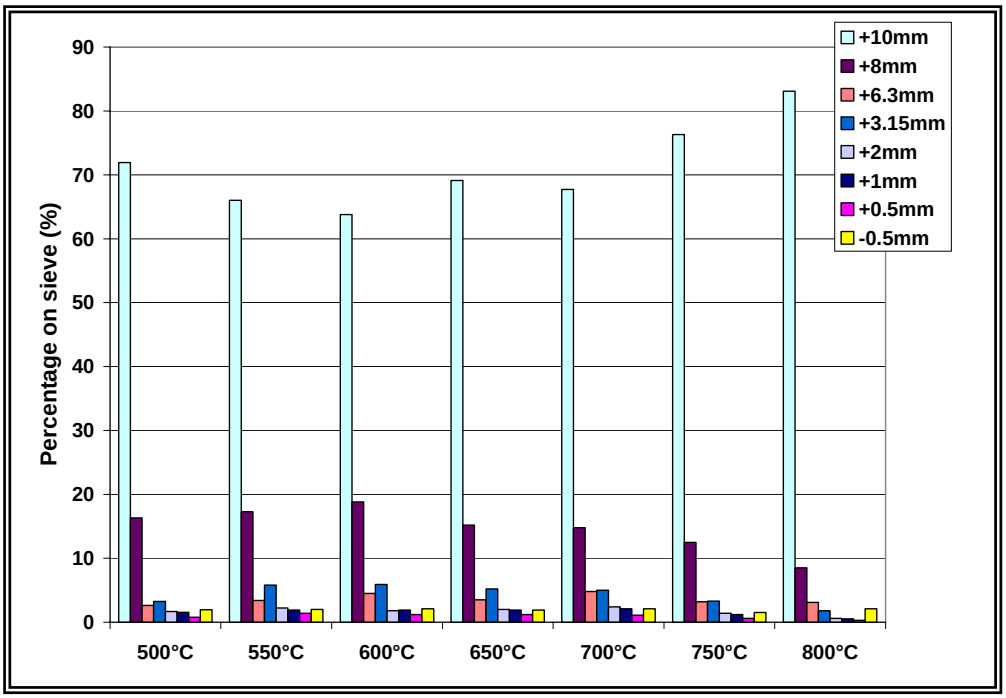

Figure 42: Effect of temperature on the reduction disintegration of Northern Cape STD. The burden was -12.5+10mm and the reduction time 60 minutes.

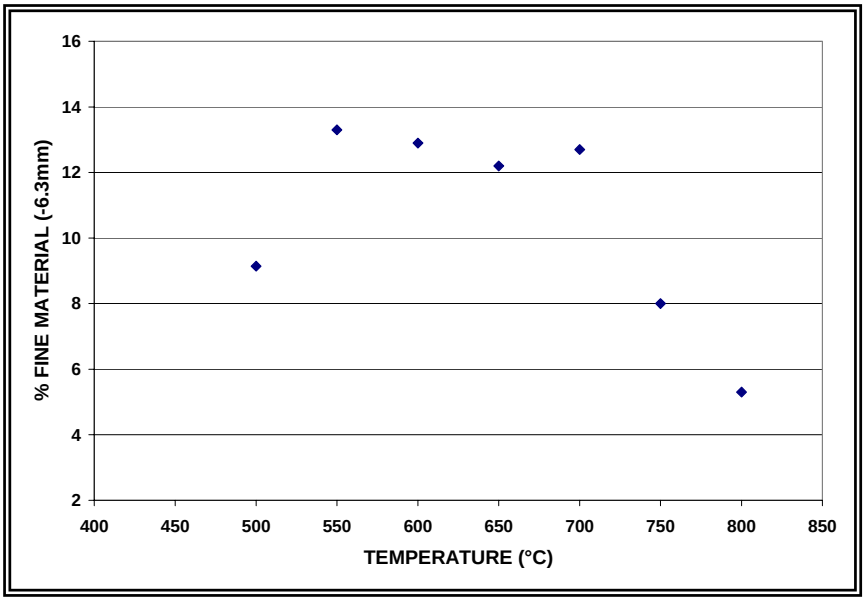

Figure 43: Effect of Temperature on the reduction disintegration of Northern Cape STD

3.2 EVALUATION OF CRACK FORMATION AND PROPAGATION

As shown by the results presented in the previous section, Northern Cape OT 4 has the lowest low temperature breakdown, while Northern Cape OT 2 gave the most low temperature breakdown. **Figure 44** - **Figure 59** are SEM images of the typical occurrences of cracks for the different size fractions after reduction disintegration for these two ore types. All of these images were obtained using back-scattered electron imaging. The brightest regions are iron oxide, the black regions mounting resin or pores and the grey regions gangue.

The results regarding crack association with gangue are given in **Table 13 – Table 17** for the individual samples with graphical representation of the results in **Figure 60 - Figure 64.**

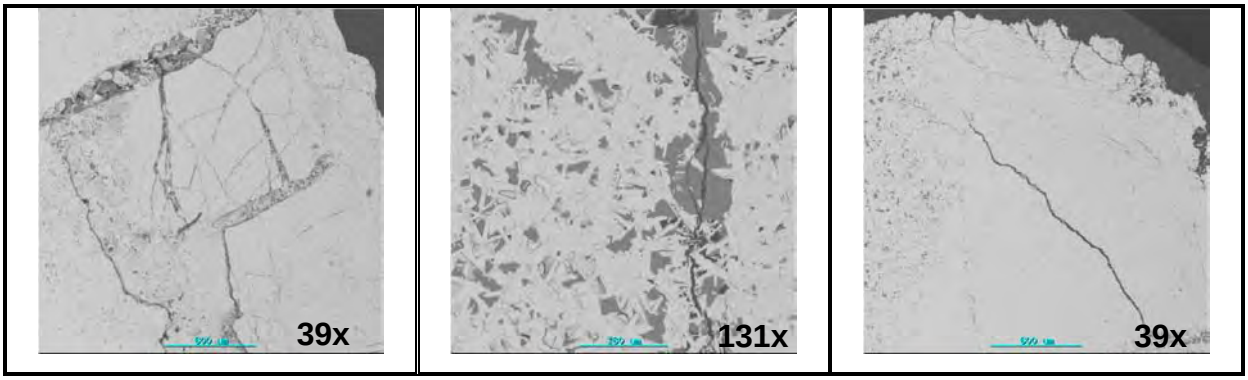

Figure 44: SEM images of the -12+10mm fraction after reduction disintegration test for Northern Cape OT 2.

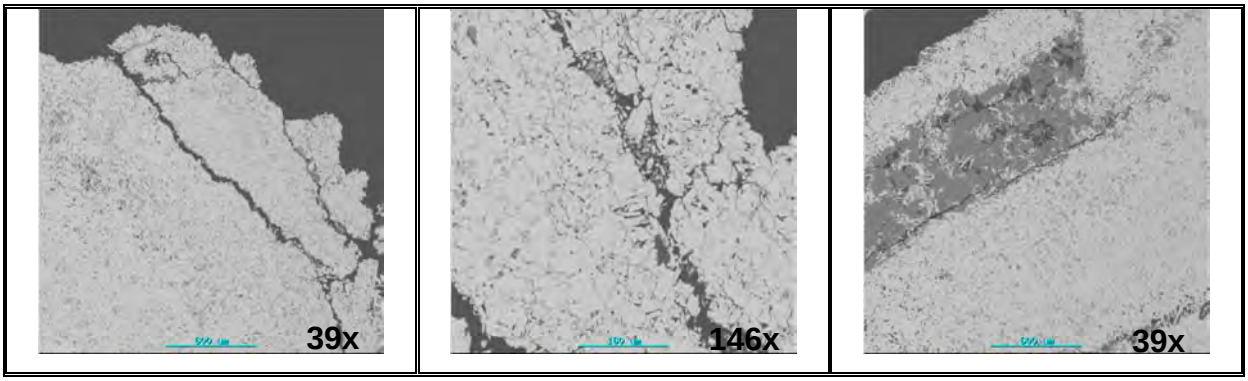

Figure 45: SEM images of the -10+8mm fraction after reduction disintegration test for Northern Cape OT 2.

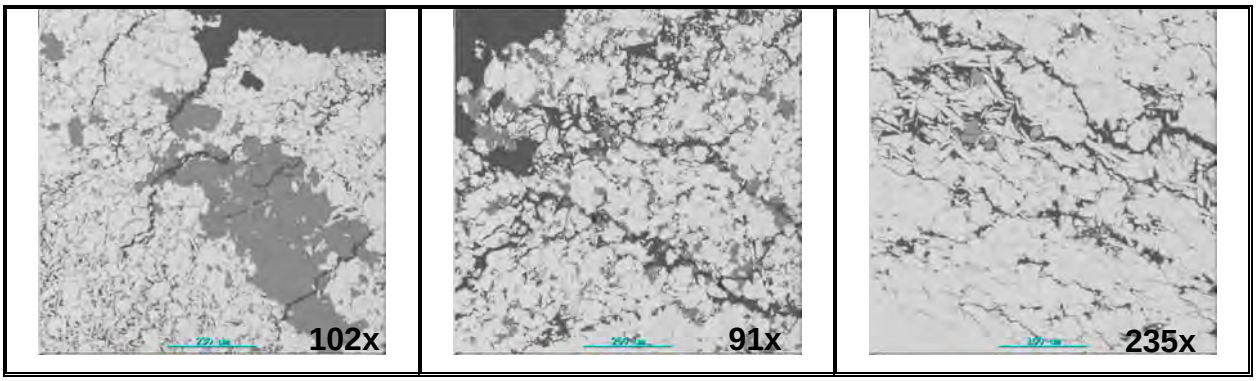

Figure 46: SEM images of the -8+6.3mm fraction after reduction disintegration test for Northern Cape OT 2.

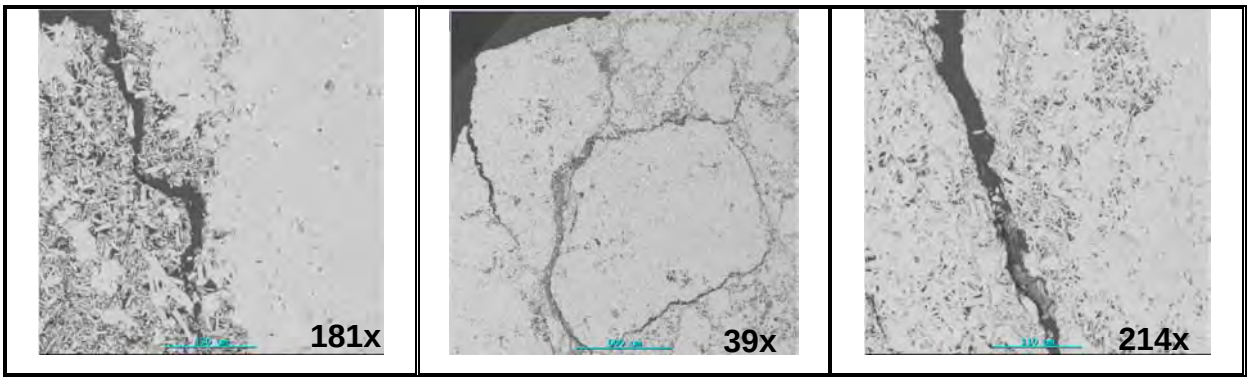

Figure 47: SEM images of the -6.3+3.15mm fraction after reduction disintegration test for Northern Cape OT 2.

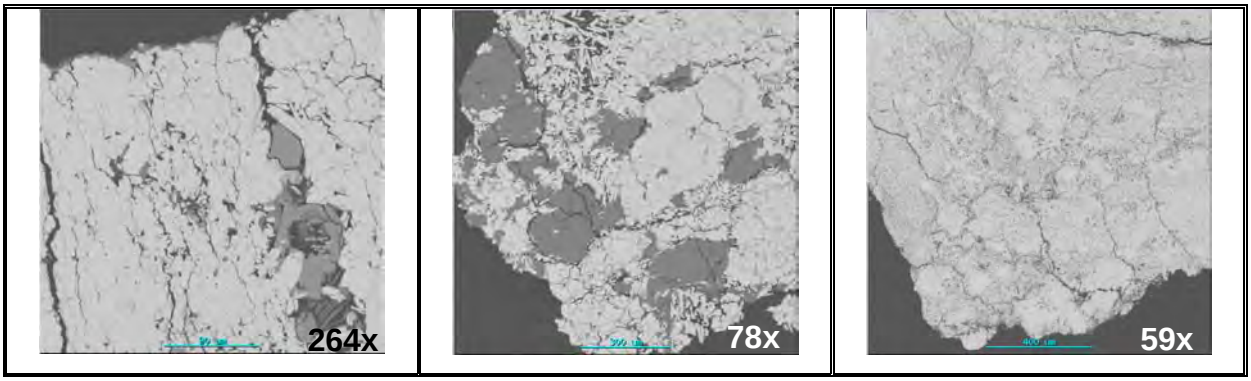

Figure 48: SEM images of the -3.15+2mm fraction after reduction disintegration test for Northern Cape OT 2.

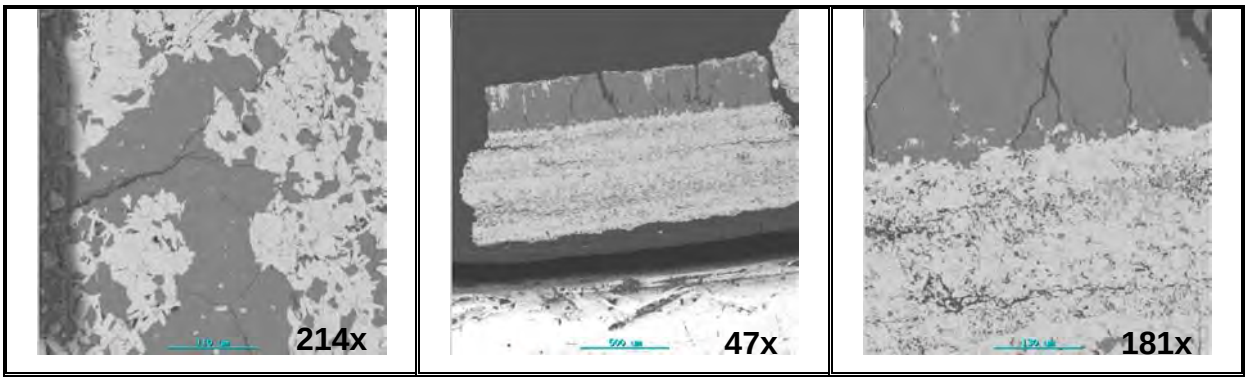

Figure 49: SEM images of the -2+1mm fraction after reduction disintegration test for Northern Cape OT 2.

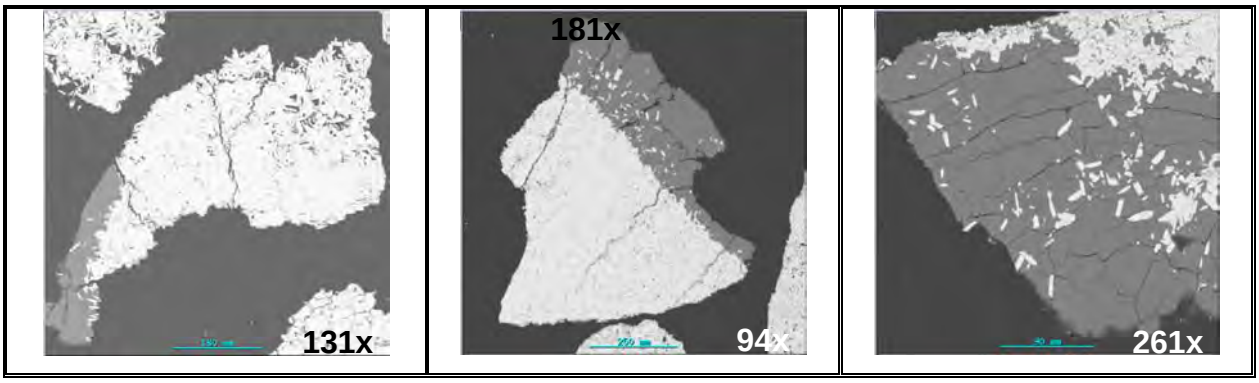

Figure 50: SEM images of the -1+0.5mm fraction after reduction disintegration test for Northern Cape OT 2.

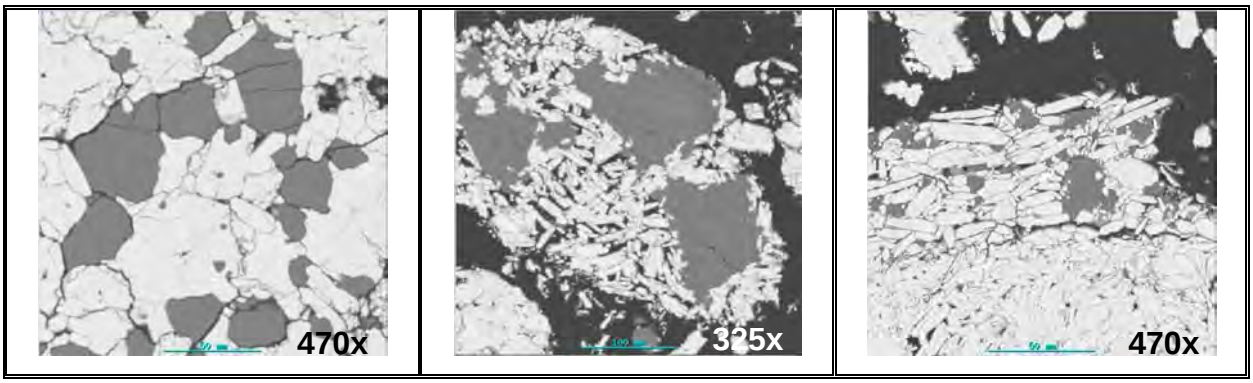

Figure 51: SEM images of the -0.5mm fraction after reduction disintegration test for Northern Cape OT 2.

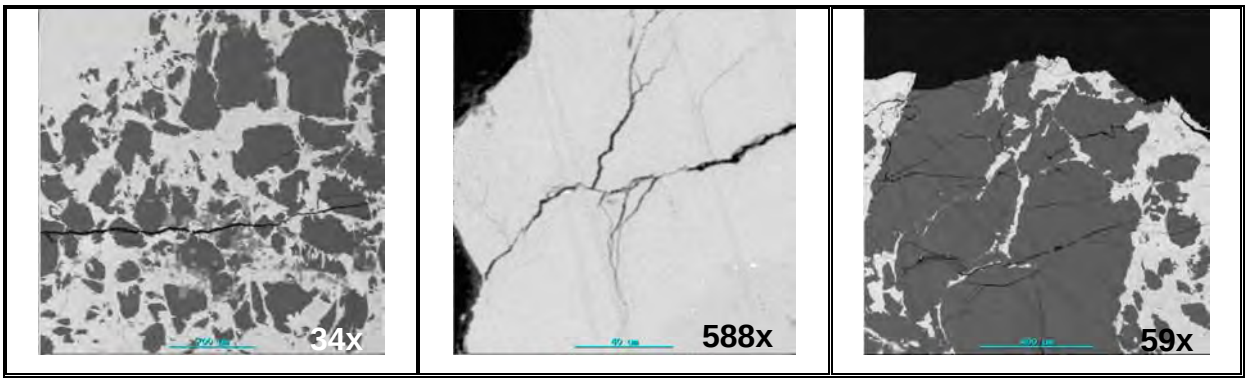

Figure 52: SEM images of the -12+10mm fraction after reduction disintegration test for Northern Cape OT 4.

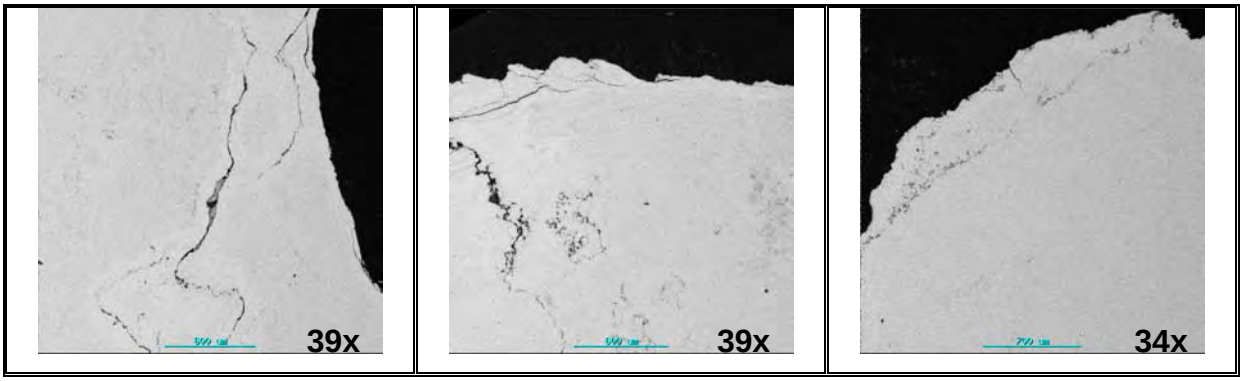

Figure 53: SEM images of the -10+8mm fraction after reduction disintegration test for Northern Cape OT 4.

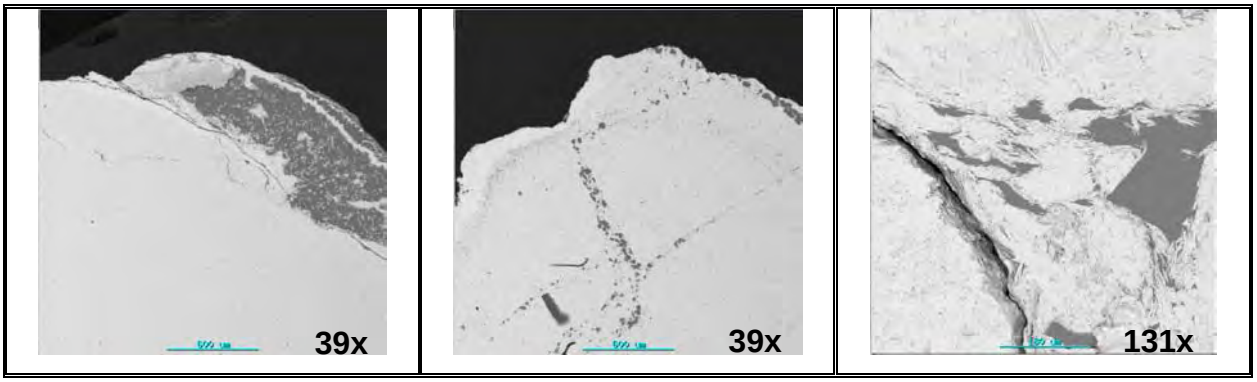

Figure 54: SEM images of the -8+6.3mm fraction after reduction disintegration test for Northern Cape OT 4.

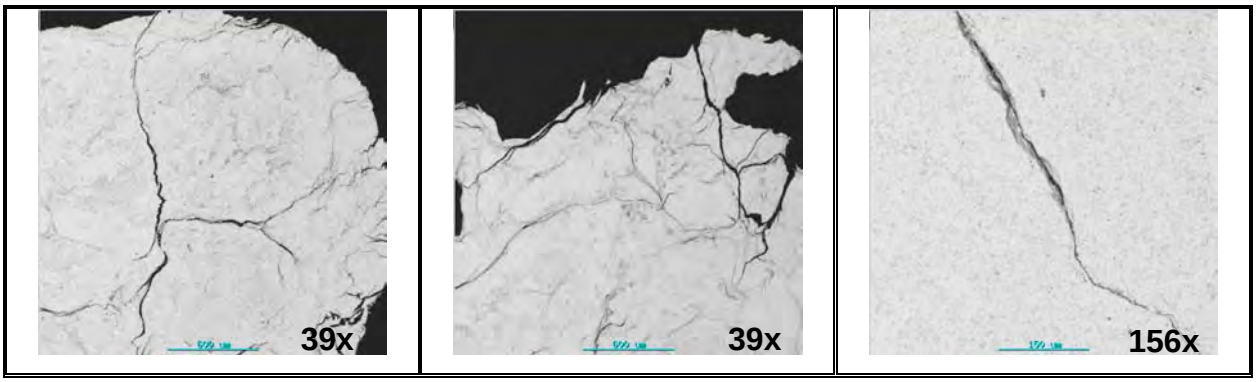

Figure 55: SEM images of the -6.3+3.15mm fraction after reduction disintegration test for Northern Cape OT 4.

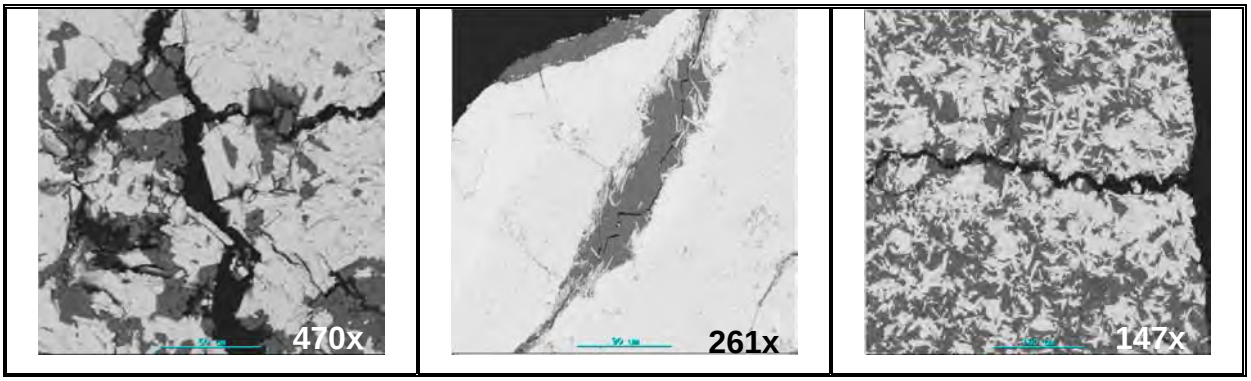

Figure 56: SEM images of the -3.15+2mm fraction after reduction disintegration test for Northern Cape OT 4.

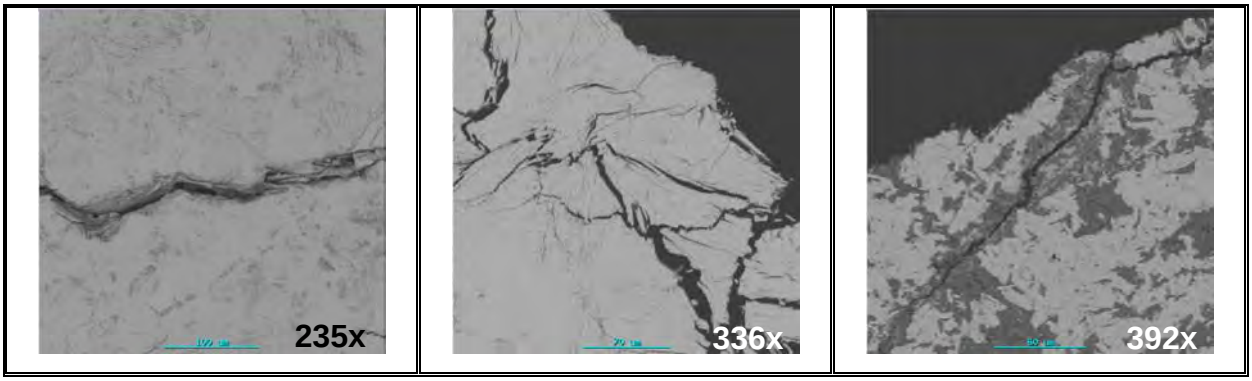

Figure 57: SEM images of the -2+1mm fraction after reduction disintegration test for Northern Cape OT 4.

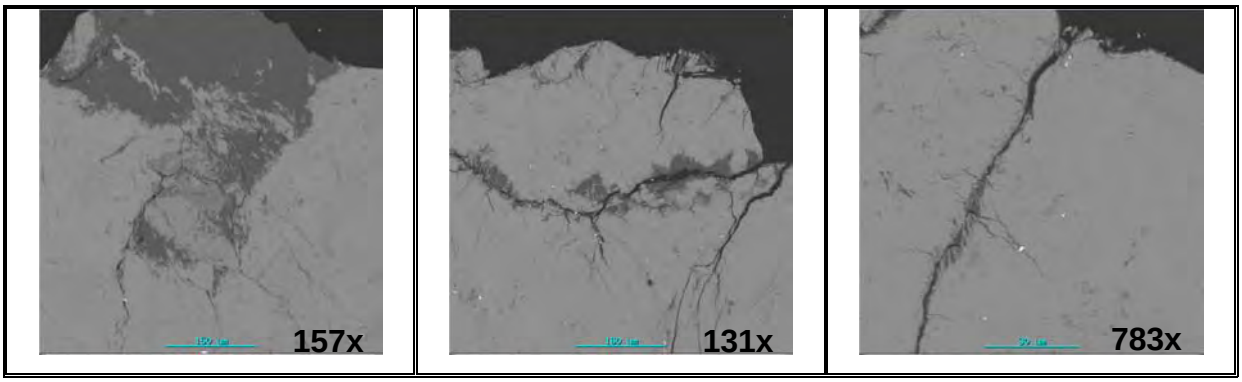

Figure 58: SEM images of the -1+0.5mm fraction after reduction disintegration test for Northern Cape OT 4.

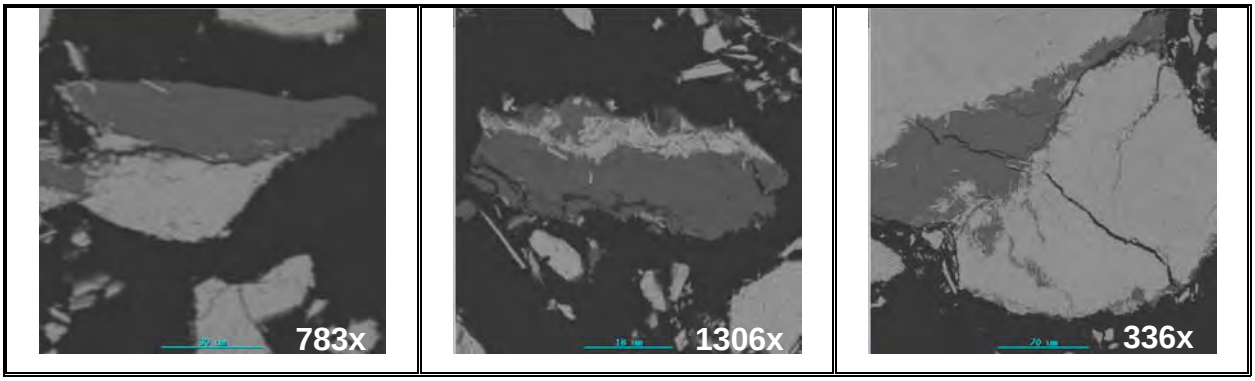

Figure 59: SEM images of the -0.5mm fraction after reduction disintegration test for Northern Cape OT 4.

Table 13: Crack association in the different size fractions of Northern Cape STD (-10+8mm) as determined from SEM images.

Size Fraction,mm	Image Ref No.	% Cracks assoc. with iron oxide	%Cracks assoc. with gangue	% v/v Gangue	% v/v iron oxide
-6.3 + 3.15	B	100	0	4	96
-6.3 + 3.15	C	82	18	23	87
-10 + 8	P	15	85	34	66
-10 + 8	Q	90	10	42	58

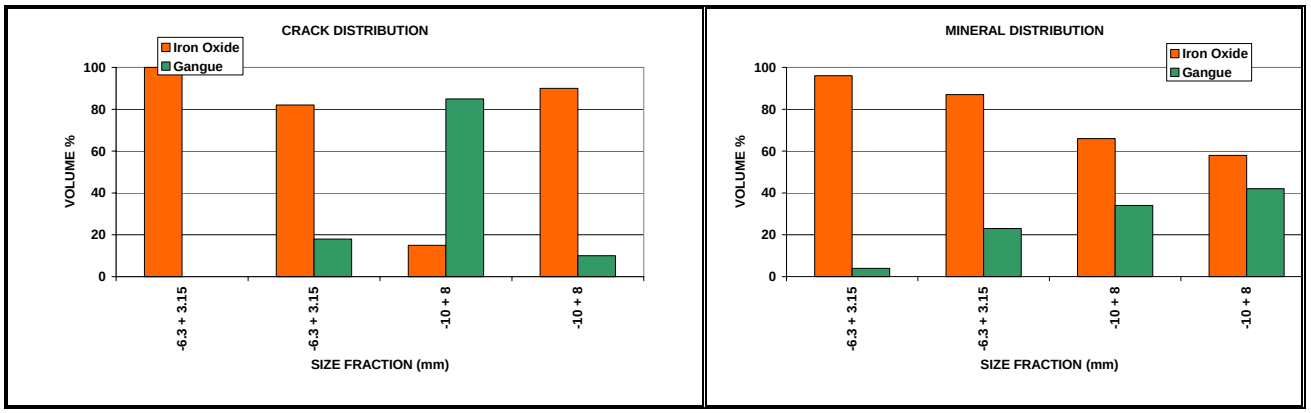

Figure 60: Graphical representation of crack association in the different size fractions of Northern Cape STD (-10+8mm).

Table 14: Crack association in the different size fractions of Northern Cape OT 2 as determined from SEM images.

Size Fraction,mm	Image Ref No.	% Cracks assoc. with iron oxide	%Cracks assoc. with gangue	% v/v Gangue	% v/v iron oxide
-0.5	1.1.1_1	69	31	20	80
-0.5	2.1.1_1	76	24	14	86
-0.5	3.1.1_1	71	29	15	85
-0.5	5.1.1_1	82	18	11	89
-0.5	9.1.1_1	59	41	25	75
-1 + 0.5	1.1.1_2	98	2	6	94
-1 + 0.5	5.1.1_1	100	0	0	100
-1 + 0.5	7.1.1_1	85	15	7	93
-1 + 0.5	9.1.1_1	100	0	5	95
-2 + 1	5.1.1_1	100	0	2	98
-3.5 + 2	2.1.1_1	72	28	22	78
-6.3 + 3.15	1.1.1_1	100	0	0	100
-6.3 + 3.15	3.1.1_1	87	13	30	70
-10+ 8	1.1.1_1	100	0	0	100
-10+ 8	2.1.1_1	83	17	20	80
-12 + 10	1.1.1_1	89	11	17	83
-12 + 10	1.5.1_1	87	13	9	91
-12 + 10	3.3.1_1	91	9	11	89

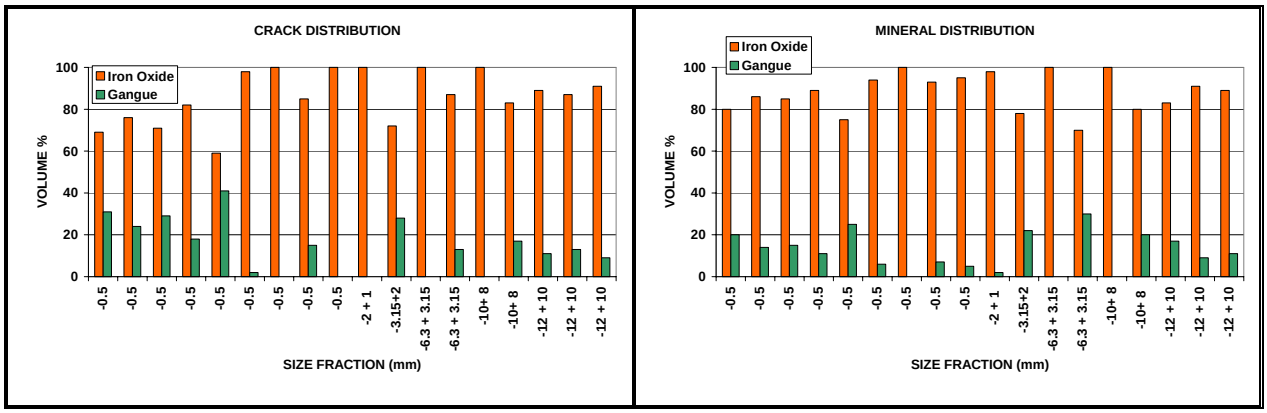

Figure 61: Graphical representation of crack association in the different size fractions of Northern Cape OT 2.

Table 15: Crack association in the different size fractions of Northern Cape OT 4 as determined from SEM images.

Size Fraction,mm	Image Ref No.	% Cracks assoc. with iron oxide	%Cracks assoc. with gangue	% v/v Gangue	% v/v iron oxide
-12.5 + 10	2.10.1_1	20	80	27	73
-12.5 + 10	2.2.1_1	65	35	53	47
-2+1	1.1.1_1	100	0	0	100
-2+1	6.1.1_1	74	26	35	65
-6.3+3.15	3.1.1_1	100	0	7	93

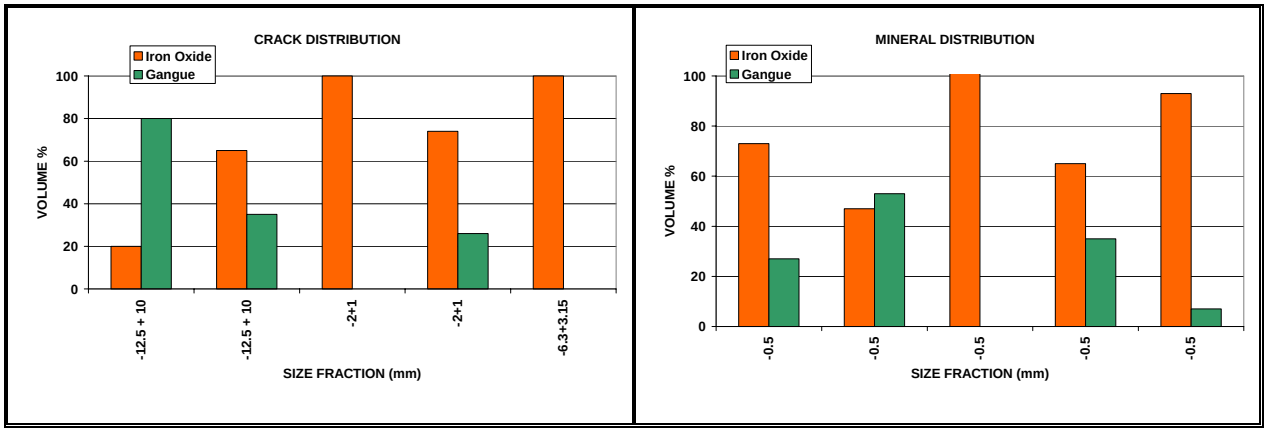

Figure 62: Graphical representation of the crack association in the different size fractions of Northern Cape OT 4.

Table 16: Crack association in the different size fractions of Northern Cape OT 5 as determined from SEM images.

Size Fraction,mm	Image Ref No.	% Cracks assoc. with iron oxide	%Cracks assoc. with gangue	% v/v Gangue	% v/v iron oxide
-0.5	1.1.1_1	97	3	8	92
-1 + 0.5	5.1.1_1	87	13	17	83
-1 + 0.5	8.1.1_1	72	28	35	75
-2+1	10.1.1_1	29	71	80	20
-2+ 1	12.1.1_1	86	14	10	90
-3.15 + 2	1.1.1_1	83	17	25	75
-3.15+ 2	5.2.2_1	61	39	28	72
-10+8	1.5. 1_1	68	32	35	75
-12+10	2.1.1_1	77	23	18	82

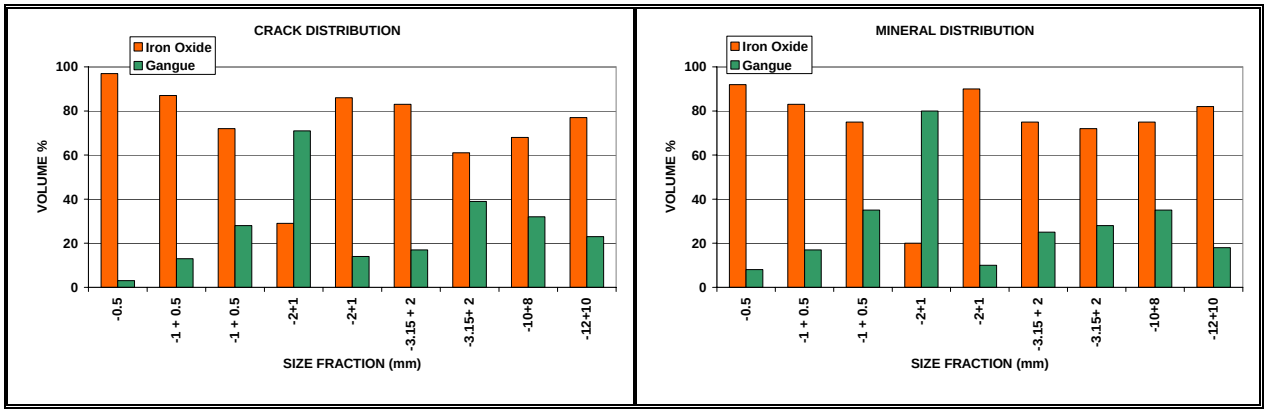

Figure 63: Graphical representation of the crack association in the different size fractions of Northern Cape OT 5.

Table 17: Results of the crack association in the different size fractions of Northern Cape OT 6 as determined from SEM images.

Size Fraction,mm	Image No.	% Cracks assoc. with iron oxide	%Cracks assoc. with gangue	% v/v Gangue	% v/v iron oxide
-0.5	4.1.1_1	84	16	30	70
-1 + 0.5	4.1.1_1	89	11	22	78
-2 +1	6.1.1_1	85	15	29	71
-3.5+ 2	10.1.1_1	73	27	38	62
-6.3+ 3.15	1.2.1_1	71	29	25	75
-8+ 6.3	1.2.1_1	75	25	27	73
-10+ 8	3.3.2_1	100	0	6	94

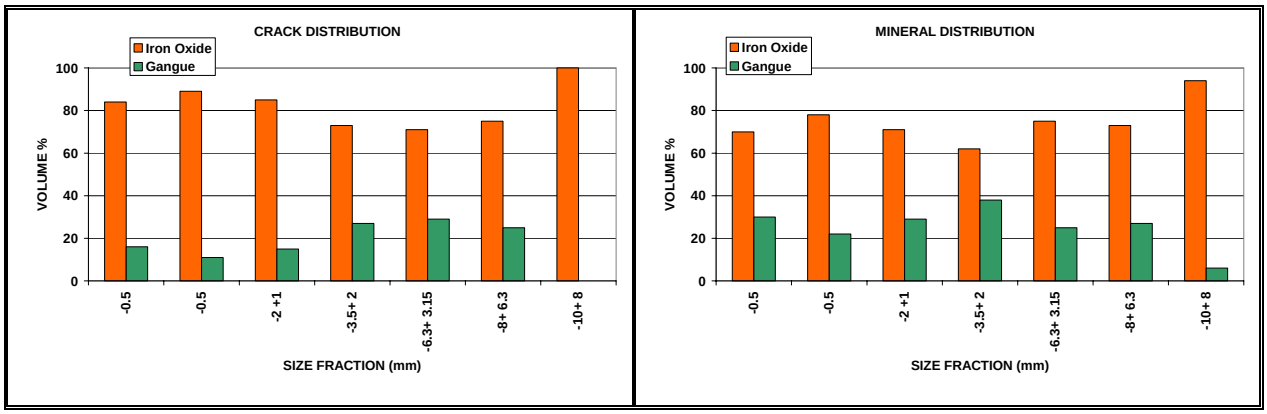

Figure 64: Graphical representation of the crack association in the different size fractions of Northern Cape OT 6.

3.3 HIGH TEMPERATURE MICROSCOPE REDUCTION TESTS

During the high temperature test a video recording was made for the duration of the test. This was evaluated afterwards for crack generation and propagation. During three of the tests the first crack was generated during the warming up cycle. The rest of the tests indicated that the first crack only appears 12-30 minutes after the reduction gas has been introduced. Only one sample (sample 1) demonstrated catastrophic cracking[§§]

[§§] Catastrophic Cracking – Sample forms huge cracks and physically breaks into two ore more portions

(**Figure 65**) during the test. Most of the samples cracked only once. Volume expansion was noticed in the form of cracks widening after the initial cracking took place.

Propagation of a crack was only observed in one sample (Sample 16). To confirm these initial results, the test was repeated under an inert atmosphere. No cracking was observed. The reduction time was also increased to see whether new cracking (due to increased reduction at the crack face) would commence after a while. However, the same tendency as in the original tests was observed. The influence of reduction gas and temperature on the crack formation and propagation was also tested by using H_2 as the reduction gas (Test 18-20) and increasing the temperature to 700ºC (Test 21). The data captured on video was evaluated and the cracks were defined as "large" cracks (Cracks that would lead to failure during tumbling), "internal" cracks (thin/hairline cracks that would not lead to failure) and "border" cracks (cracks on the edges of sample that would cause fine particles to spall of the edges of the sample). A summary of the results of the high temperature microscope test is given in **Table 18**. **Figure 65**-**Figure 85** is optical microscope photos of the cracks observed during the tests. **Table 19** is a summary of the SEM analysis of the samples after reduction in the high temperature microscope.

Table 18: Summary of the cracks observed during and after reduction tests in high temperature microscope.

Sample No.	Sample Name	Time before 1st crack	No. of large cracks	No. of cracks growing from large cracks	Internal cracks	Border cracks
1	Northern Cape OT 5	17	3	5	6	5
2	Northern Cape OT 2	0	2	3	2	2
3	Northern Cape OT 4	15	0	0	1	3
6	Northern Cape OT 2	0	4	3	2	5
8	Northern Cape STD	26	0	0	3	2
10	Northern Cape OT 4	0	2	0	2	3
12	Northern Cape OT 2	1	1	0	1	1
13	Northern Cape	21	1	0	0	4

	STD					
14	Northern Cape OT 5	16	1	3	1	2
15	Northern Cape OT 5	12	1	2	3	6
16	Northern Cape STD	18	3	5	8	5
17	Northern Cape OT 4	12	2	0	2	3
18	Northern Cape STD	30	3	4	3	5
19	Northern Cape STD	-	0	0	0	0
20	Northern Cape STD	30	3	0	4	2
21	Northern Cape STD	34	0	0	0	2

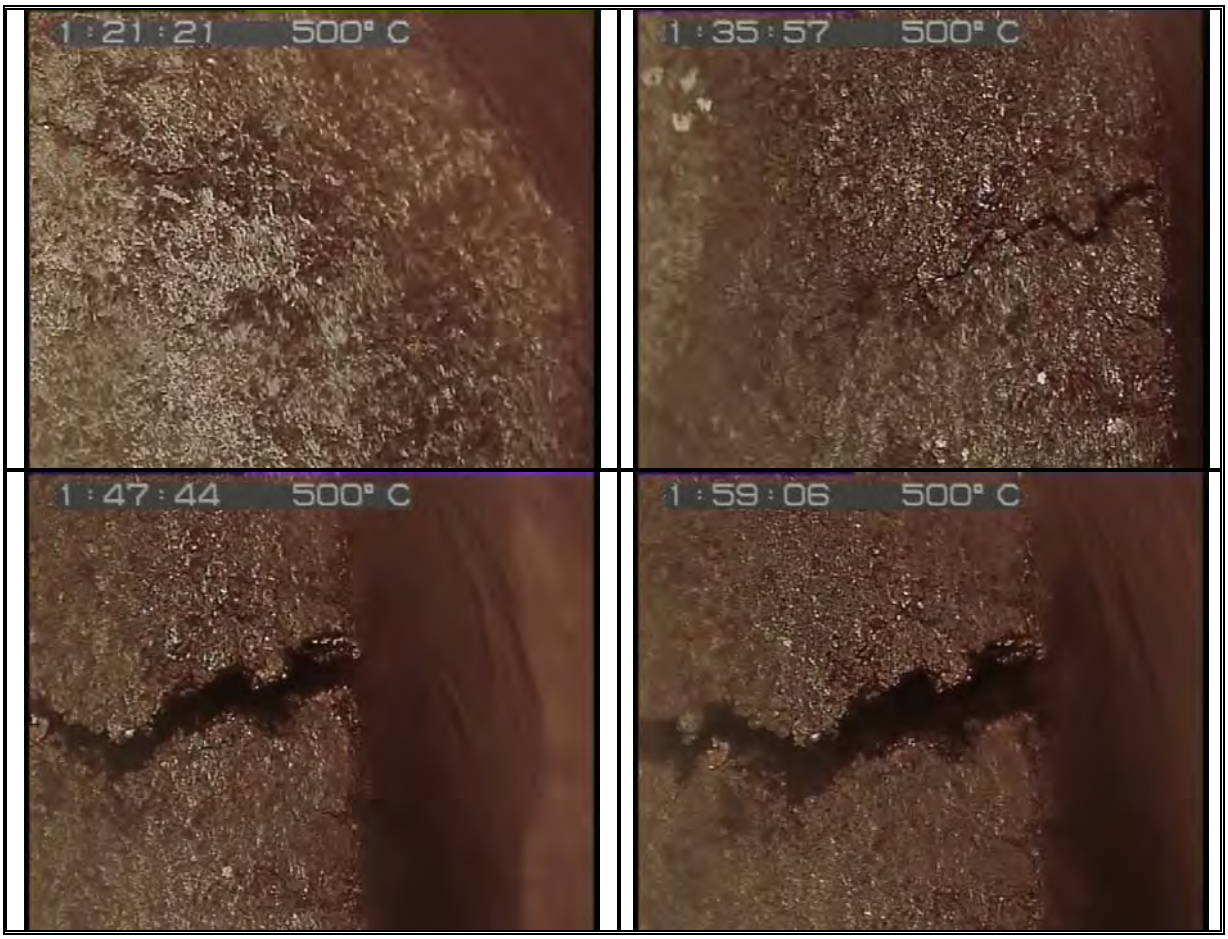

Figure 65: Optical microscope image during the high temperature microscope reduction test of Sample 1

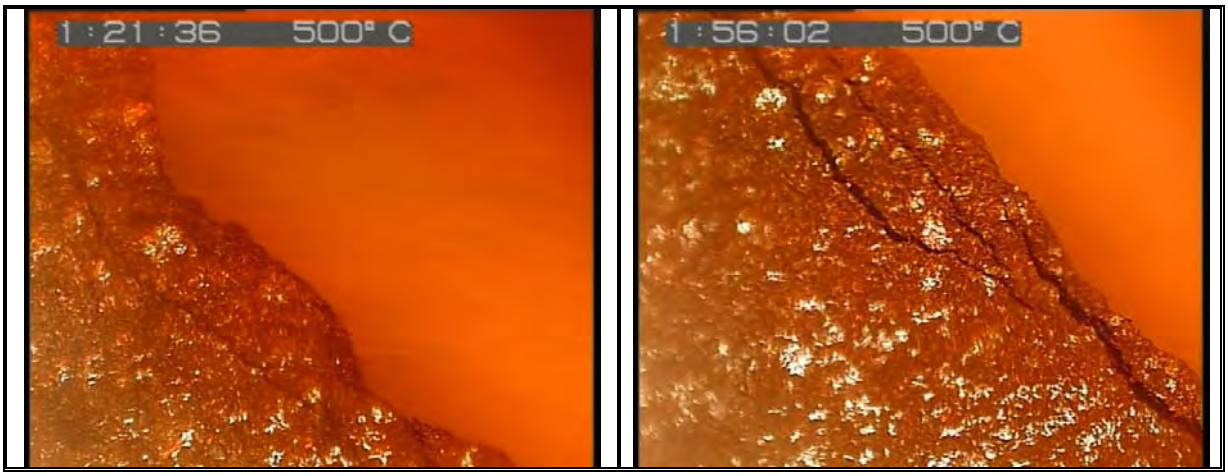

Figure 66: Optical microscope image during the high temperature microscope reduction test of Sample 13.

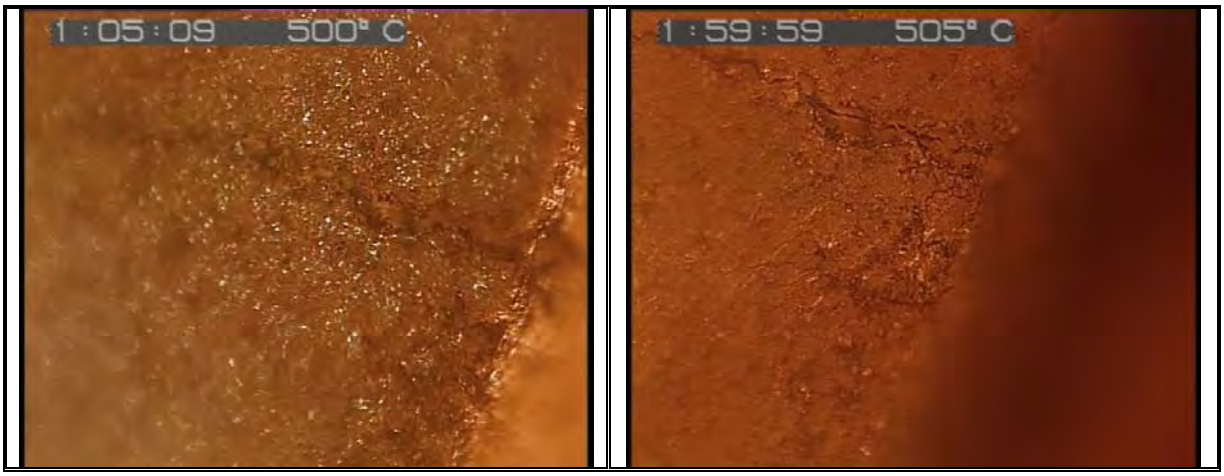

Figure 67: Optical microscope image during the high temperature microscope reduction test of Sample 14.

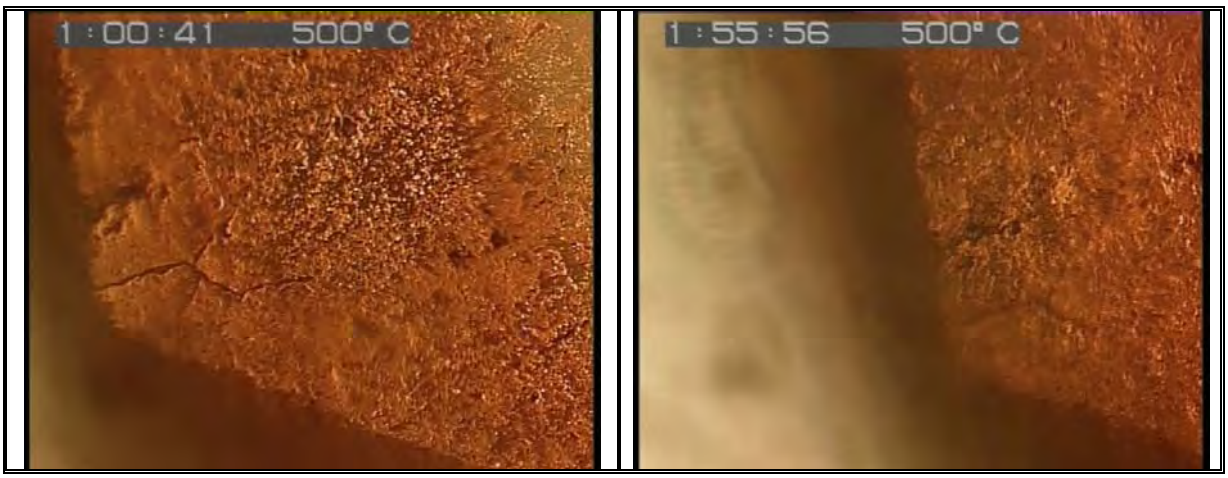

Figure 68: Optical microscope image during the high temperature microscope reduction test of Sample 15.

Figure 69: Optical microscope image during the high temperature microscope reduction test of Sample 16.

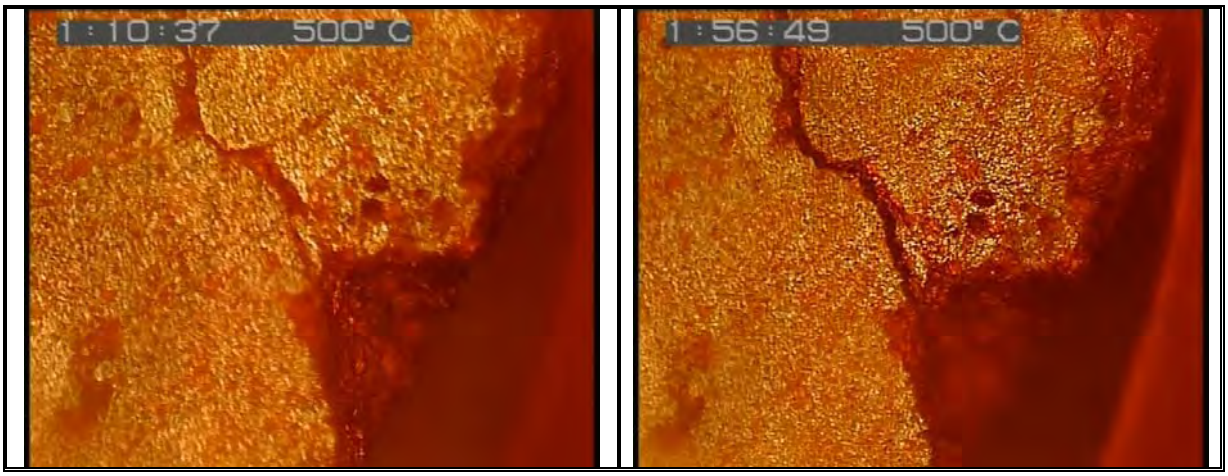

Figure 70: Optical microscope image during the high temperature microscope reduction test of Sample 16.

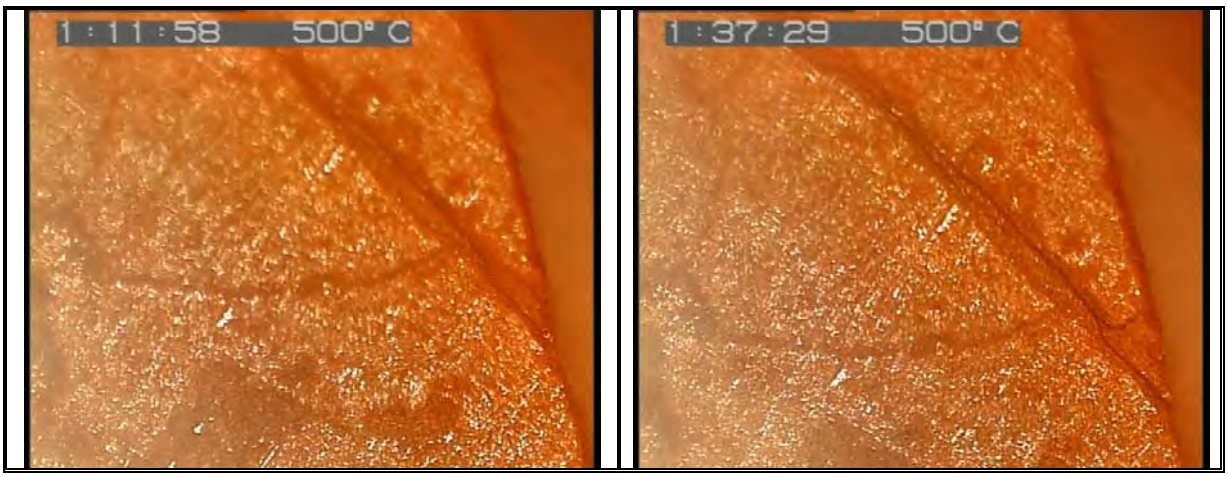

Figure 71: Optical microscope image during the high temperature microscope reduction test of Sample 17.

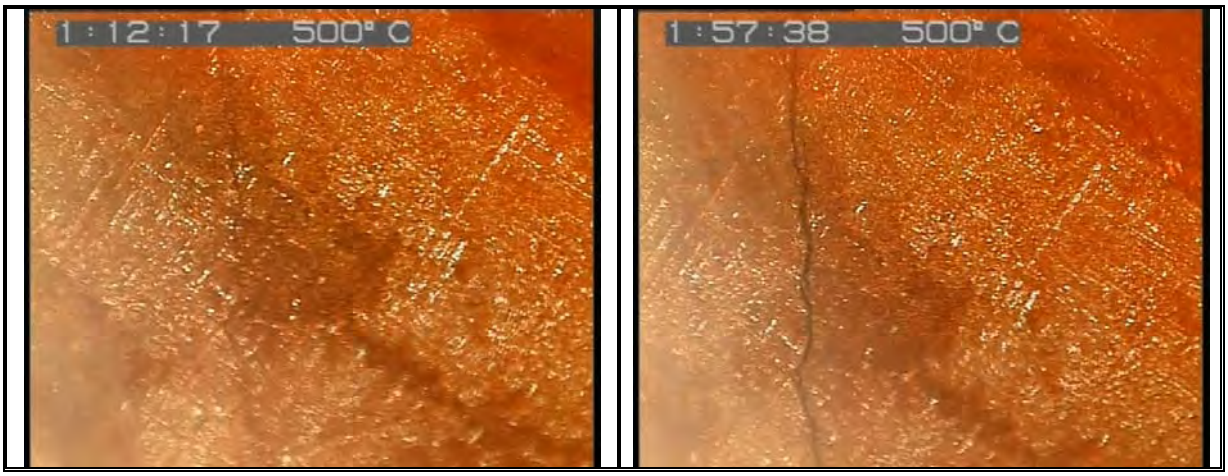

Figure 72: Optical microscope image during the high temperature microscope reduction test of Sample 17.

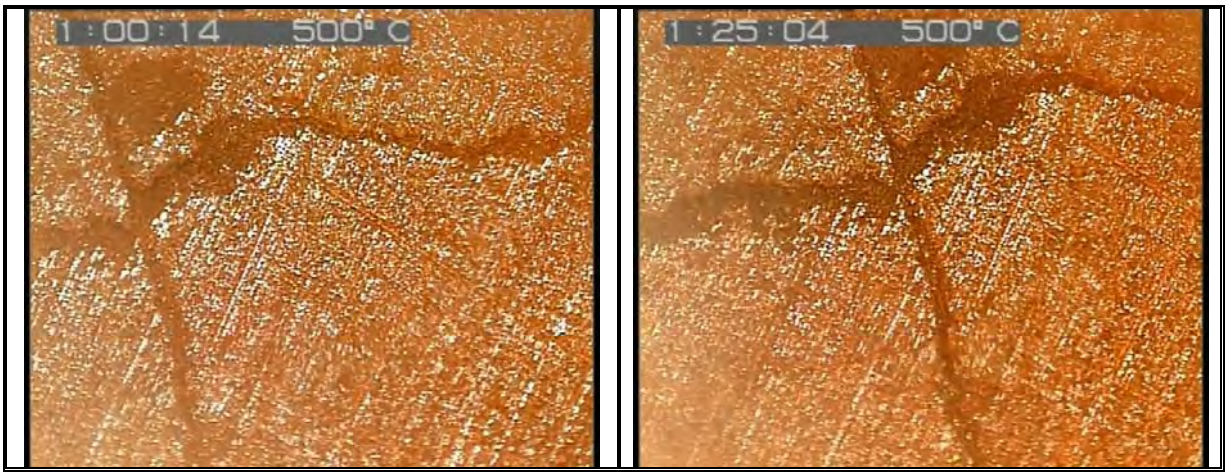

Figure 73: Optical microscope image during the high temperature microscope reduction test of Sample 17.

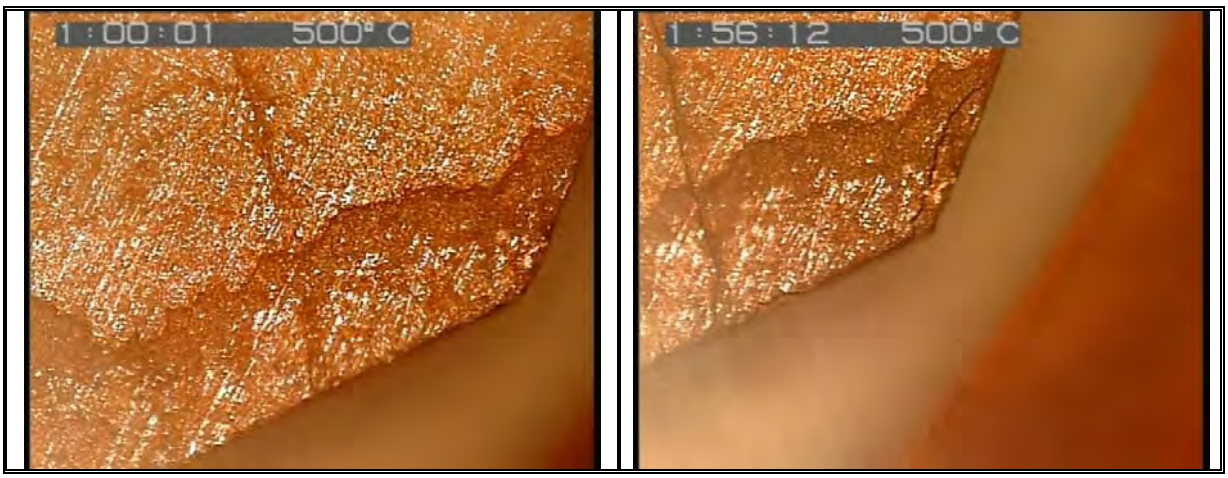

Figure 74: Optical microscope image during the high temperature microscope reduction test of Sample 17.

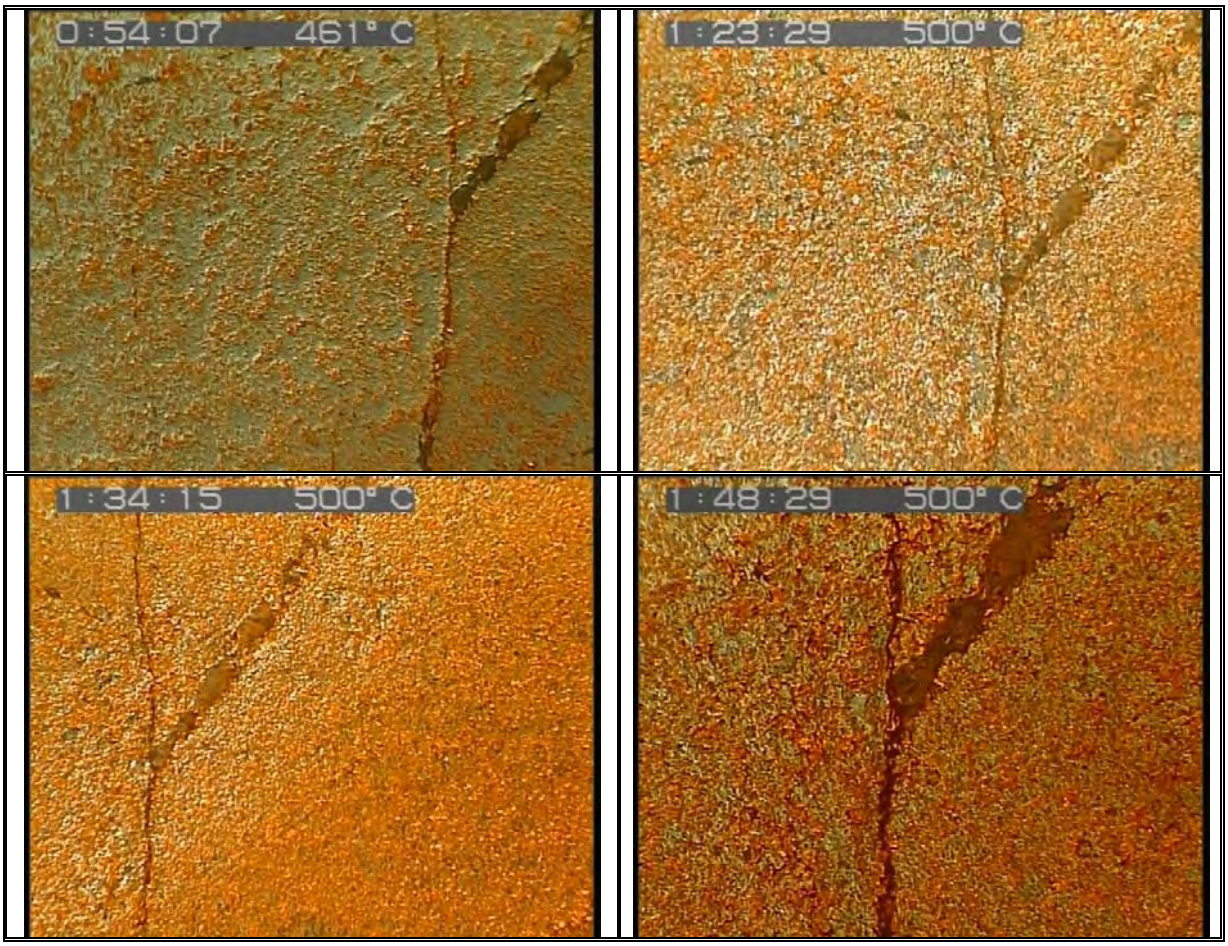

Figure 75: Optical microscope image during the high temperature microscope reduction test of Sample 18.

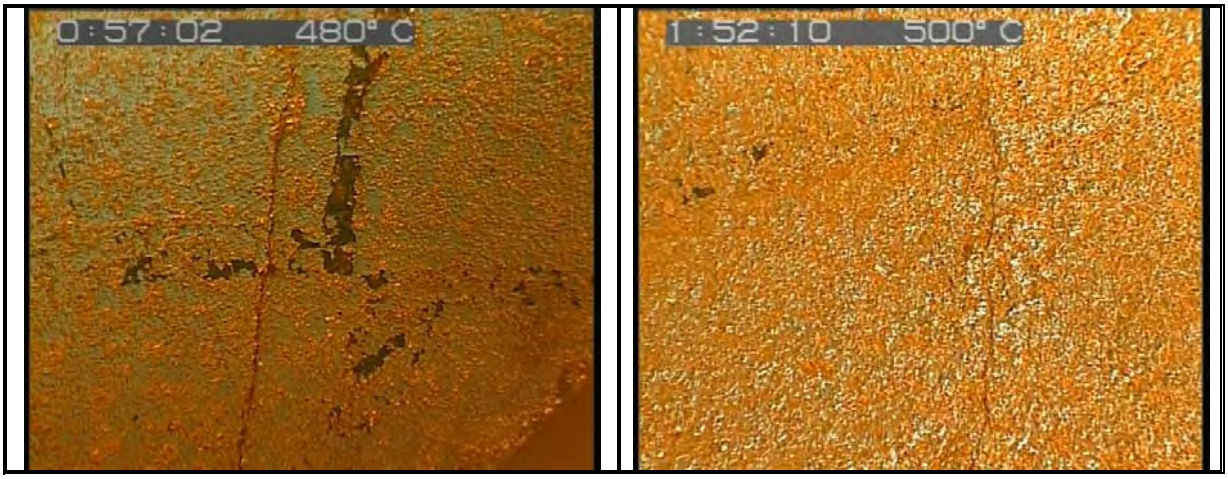

Figure 76: Optical microscope image during the high temperature microscope reduction test of Sample 18.

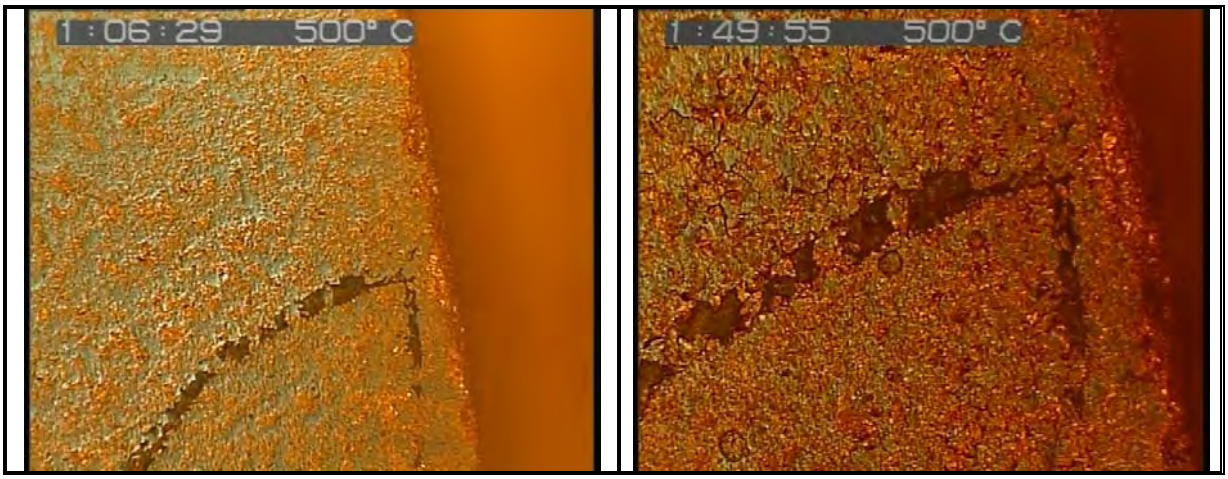

Figure 77: Optical microscope image during the high temperature microscope reduction test of Sample 18.

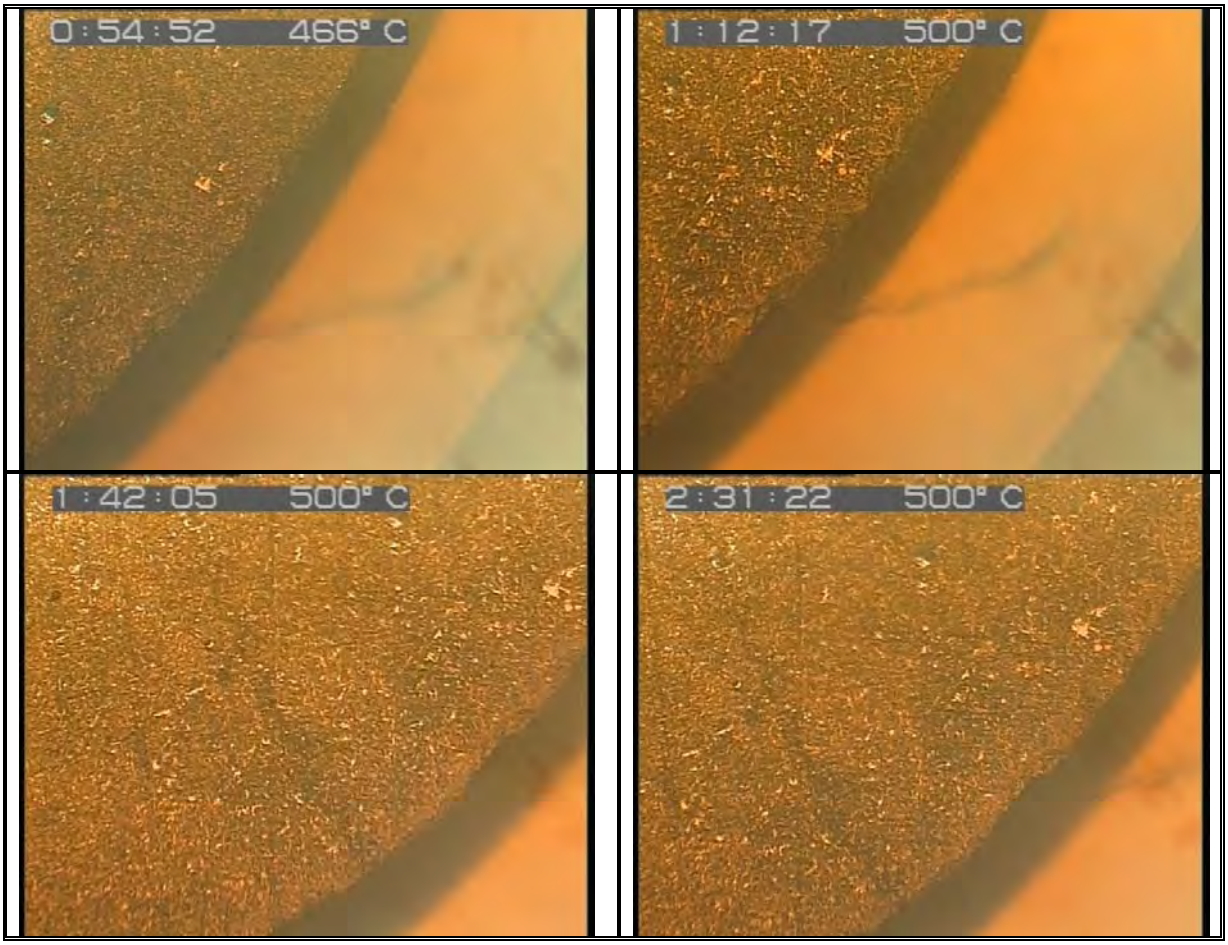

Figure 78: Optical microscope image during the high temperature microscope reduction test of Sample 19.

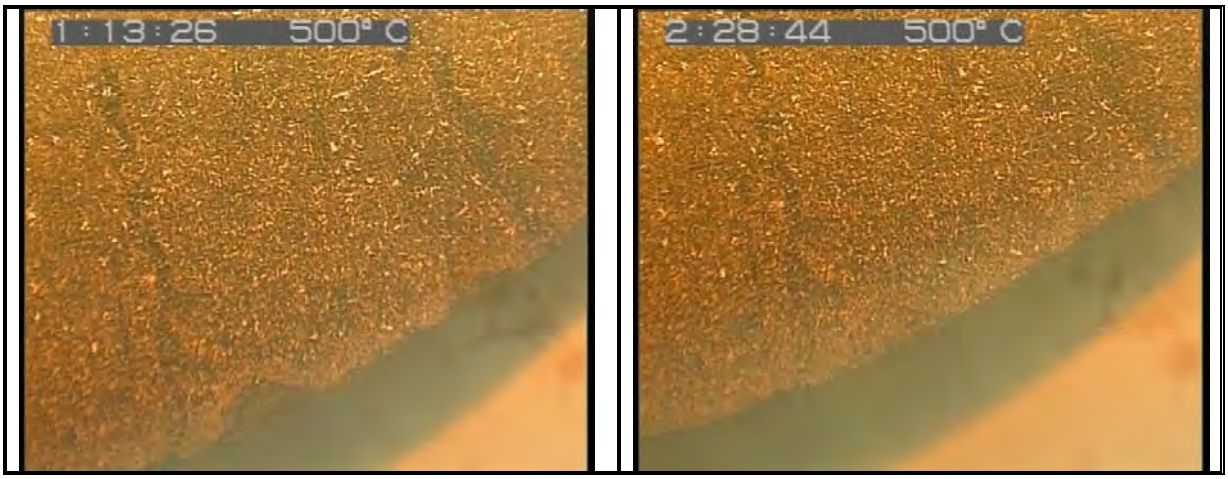

Figure 79: Optical microscope image during the high temperature microscope reduction test of Sample 19.

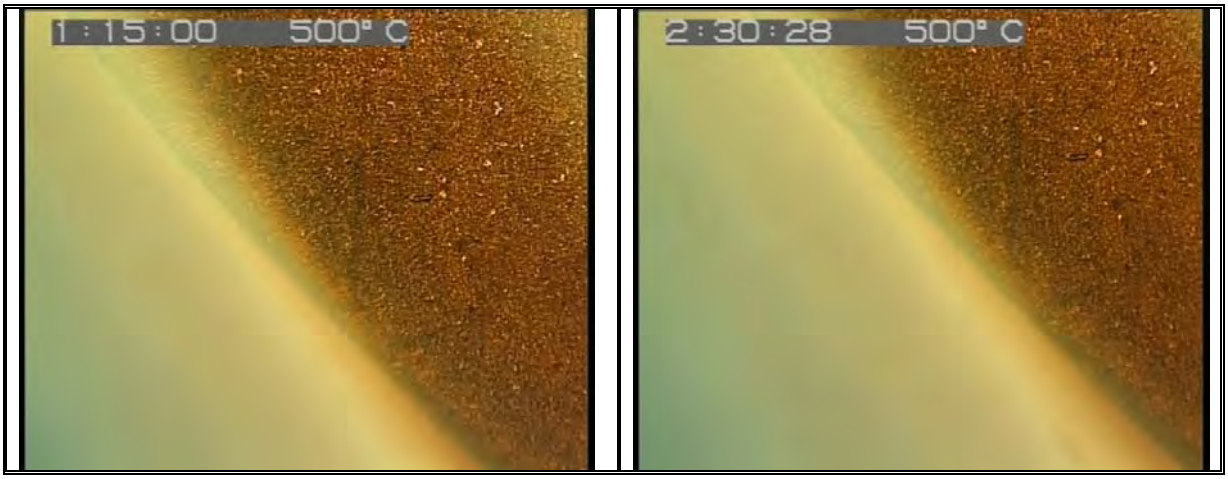

Figure 80: Optical microscope image during the high temperature microscope reduction test of Sample 19.

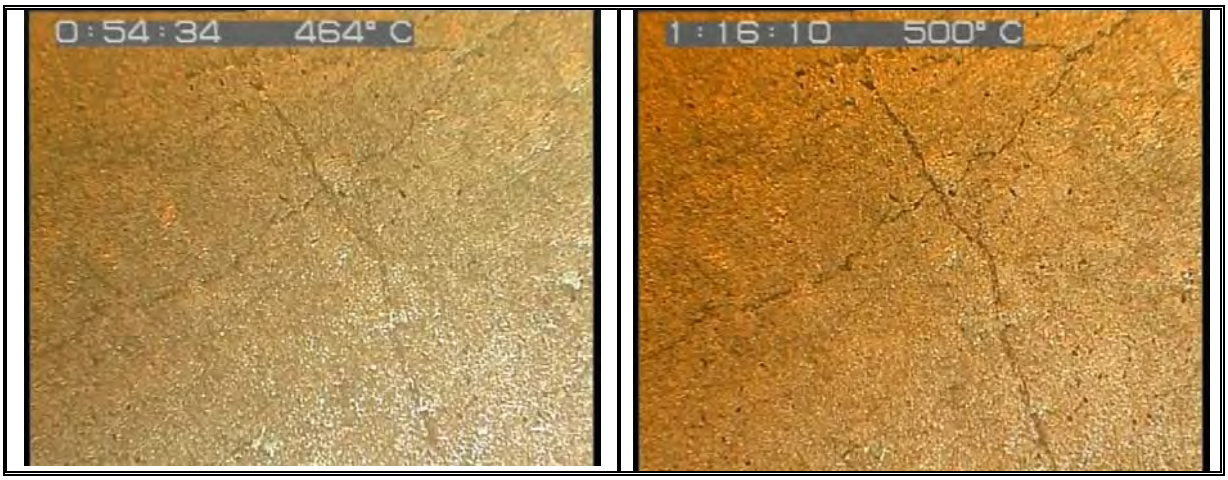

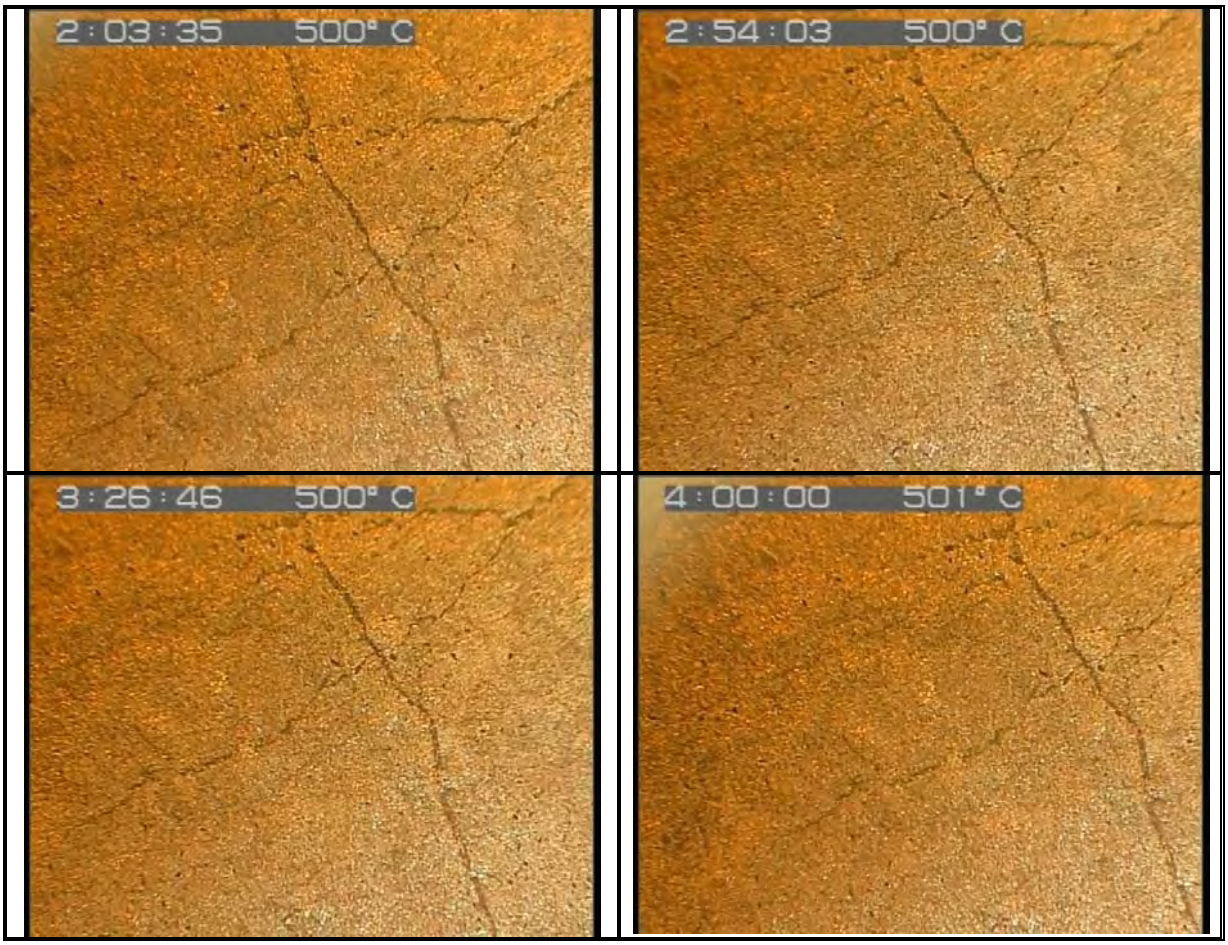

Figure 81: Optical microscope image during the high temperature microscope reduction test of Sample 20.

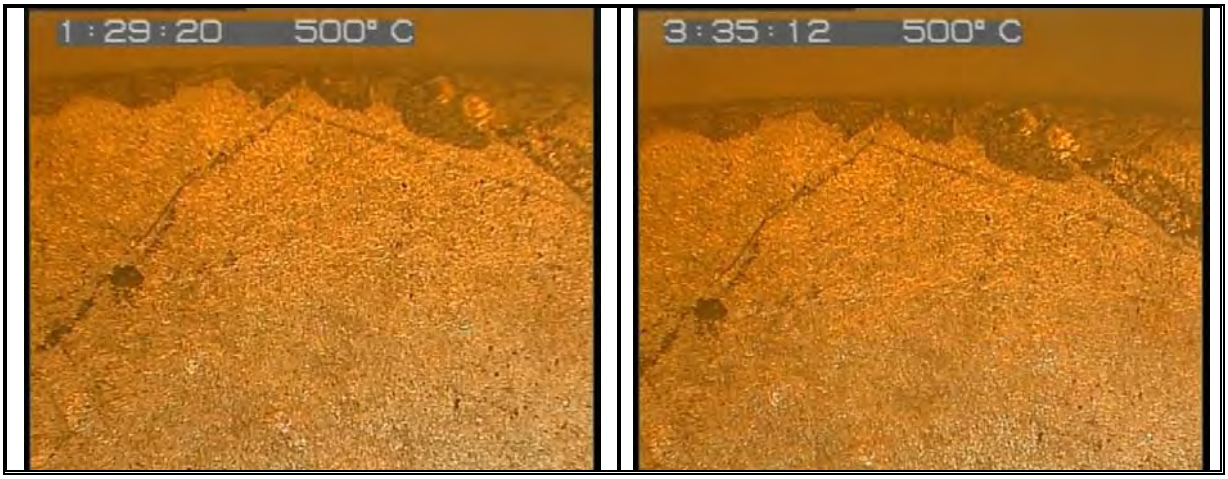

Figure 82: Optical microscope image during the high temperature microscope reduction test of Sample 20.

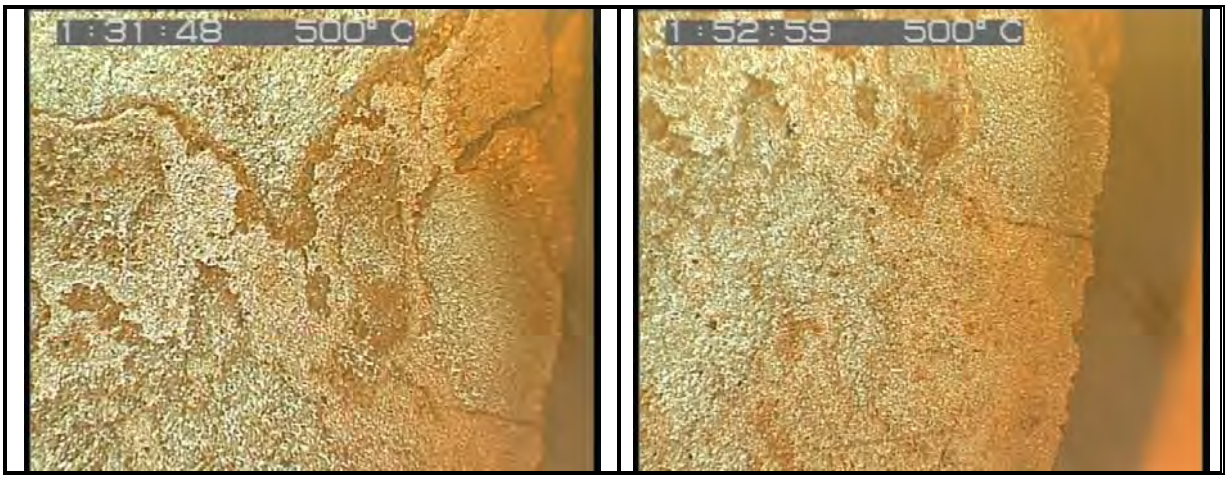

Figure 83: Optical microscope image during the high temperature microscope reduction test of Sample 20.

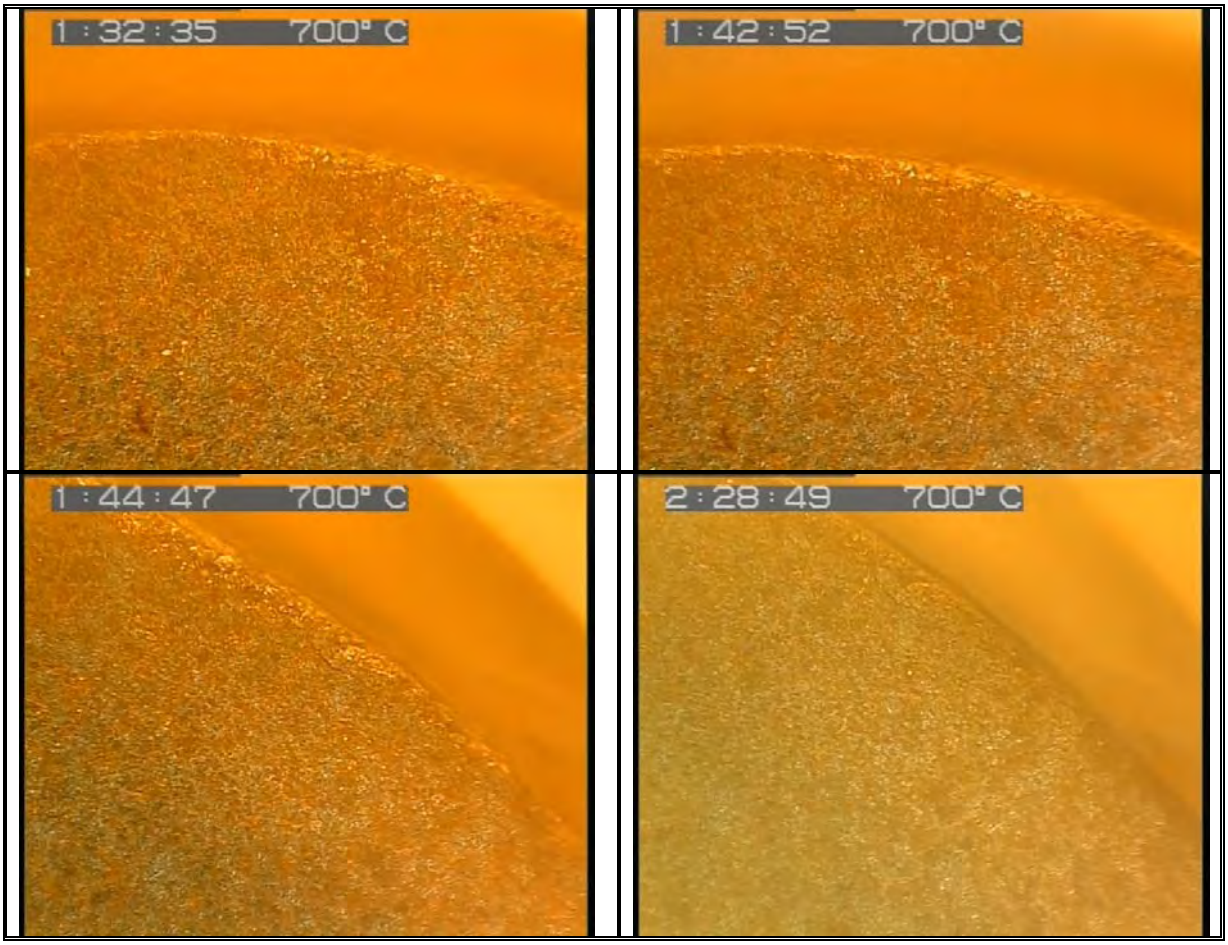

Figure 84: Optical microscope image during the high temperature microscope reduction test of Sample 21.

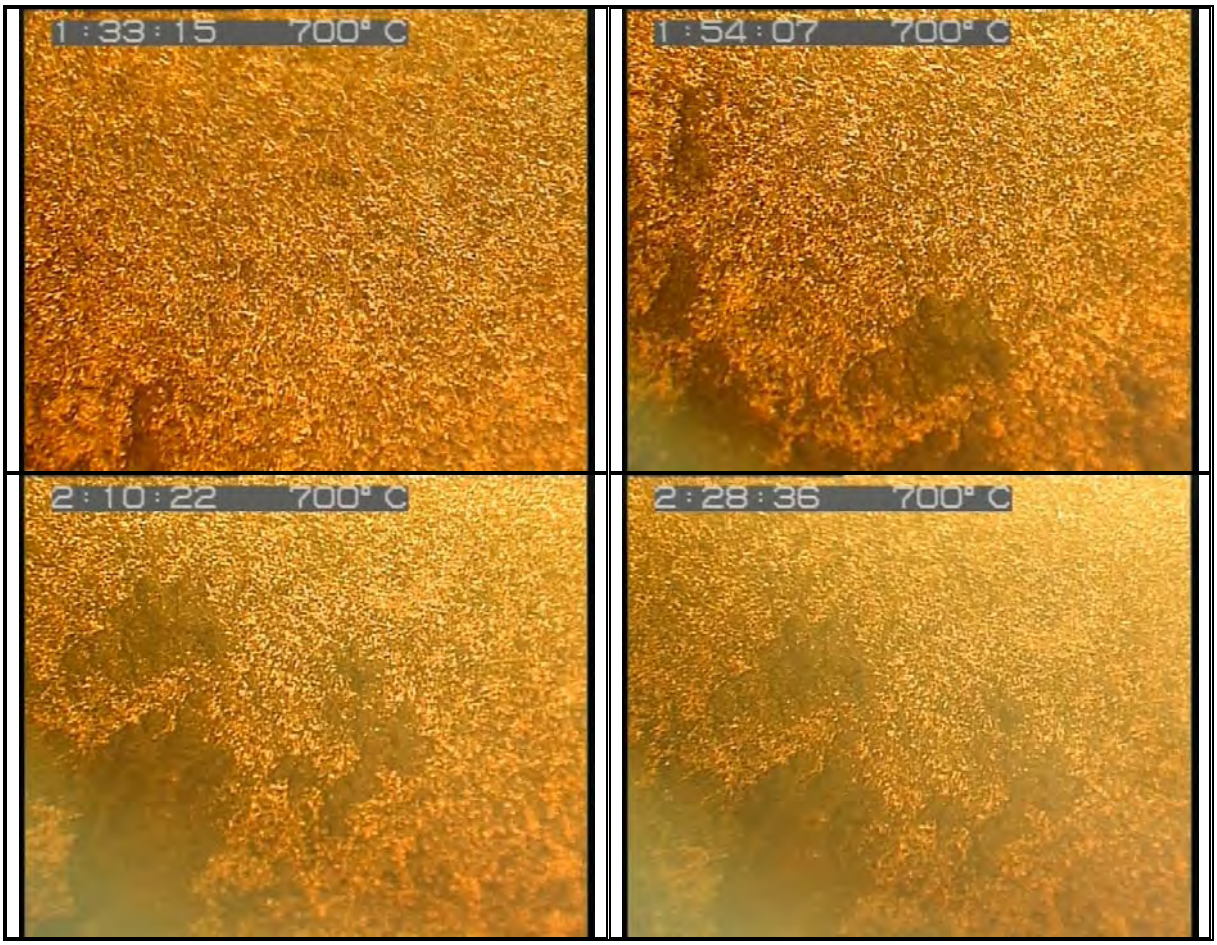

Figure 85: Optical microscope image during the high temperature microscope reduction test of Sample 21.

Table 19: Summary of SEM-analysis of iron ore samples after reduction under high temperature microscope.

Sample No.	Sample Name	Group	Gangue	Porosity	Fracture type
1	Northern Cape OT 5	Poly-mineralic samples	Apatite/Quartz	Low	Extensive, throughout the sample
2	Northern Cape OT 2	Porous	-	Variable	Regular network***
3	Northern Cape OT 4	Mono-mineralic hematite samples	-	Low	Perpendicular to edge
6	Northern Cape OT 2	Other	Quartz	Low	Parallel to foliation
8	Northern Cape STD	Mono-mineralic hematite samples	-	Low	Perpendicular to edge
10	Northern Cape OT 4	Poly-mineralic samples	Quartz/Muscovite	Low	Parallel to edge
12	Northern Cape	Mono-mineralic	-	Low	Parallel/Perpenducular

*** Regular network - network of fractures that occur at right angles to each other.

	OT 2	hematite samples			to edge
13	Northern Cape STD	Mono-mineralic hematite samples	-	Low	Parallel/Perpenducular to edge
14	Northern Cape OT 5	Poly-mineralic samples	Apatite/Quartz	Low	Parallel/Regular network to edge
15	Northern Cape OT 5	Poly-mineralic samples	Al-Silicates	Low	None
16	Northern Cape STD	Porous	-	Low	Associated with Specularite
17	Northern Cape OT 4	Mono-mineralic hematite samples	-	Low	Parallel to edge
18	Northern Cape STD	Poly-mineralic samples	Apatite/Quartz	Medium, small pores	Perpendicular/Parallel
19	Northern Cape STD	Poly-mineralic samples	Muscovite/Apatite	Low	Parallel
20	Northern Cape STD	Mono-mineralic hematite samples	Muscovite	Low	Perpendicular
21	Northern Cape STD	Mono-mineralic hematite samples	Muscovite	Small pores and large infill pores	Perpendicular/Parallel

3.4 SEM ANALYSIS

When observing samples under the SEM that have undergone deformation, with the aim of understanding the mechanisms of deformation and metamorphism, one must be mindful of the fact that the sample is only being observed in two dimensions whilst deformation has taken place in three dimensions.

In this study we only observe brittle deformation mechanisms in samples comprising predominantly of hematite with minor amounts of gangue minerals. This indicate that although the samples were between 500°C and 700°C, the stresses induced due to the reduction process taking place led to brittle cracks and that no shearing took place. **Appendix 1** list the minerals identified in this study. In this study, most samples consist predominantly of hematite and the small amount of gangue minerals present is unlikely to have an influence on the overall stress supporting network.

Each sample is discussed and described individually (**Appendix 4**). The samples were classified into four distinct groups according to the predominant feature observed in the sample. Samples were allocated into the following groups:

1. Mono-mineralic hematite samples (Samples 3, 8, 12, 13, 17, 20, 21)
2. Poly-mineralic samples (Samples 1, 10, 14, 15 18, 19)
3. Porous samples (Samples 2 and 16)
4. Other (Sample 6)

3.4.1 GROUP 1: MONO-MINERALIC HEMATITE SAMPLES

These samples consist primarily of hematite and they have very similar physical and micro-fracture characteristics. The samples have low porosity with very little or no gangue minerals present.

In these samples fractures occurs mainly perpendicular to the sample edges – the first place in which reduction occurs. The fractures only penetrate as far as the sample has been reduced. When internal fractures do occur, they are present in a network of fractures that occur at right angles to each other – commonly known as a regularly spaced framework.

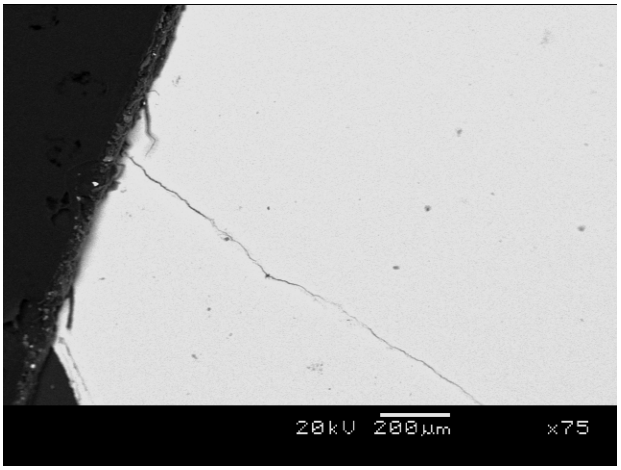

Figure 86: Electron backscatter image of sample 3 showing the homogeneity of the sample. The sample is essentially mono-mineralic and comprises almost exclusively of hematite. Small radial fractures occur at the edge of the sample, where it has been reduced.

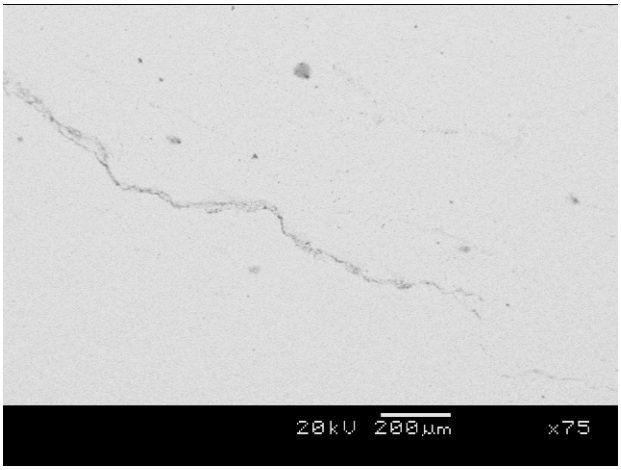

Figure 87: Electron backscatter image of sample 3 showing a rare internal fracture. This fracture is not associated with gangue minerals, porosity or reduction.

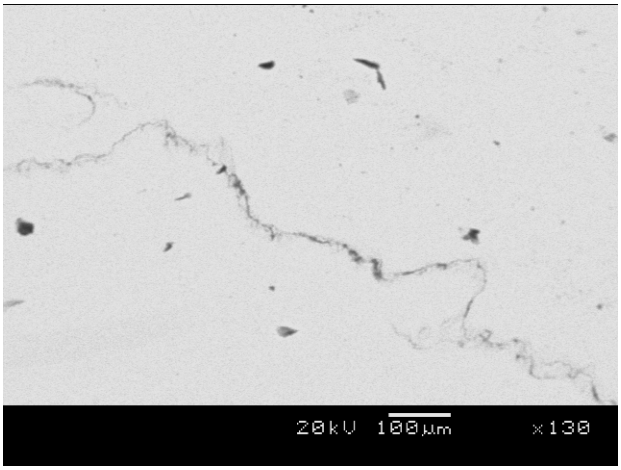

Figure 88: Electron backscatter image of sample 3 showing a pre-existing fracture filled with muscovite.

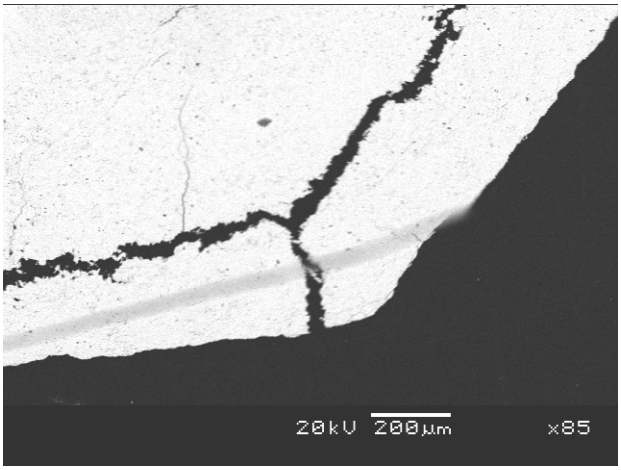

Figure 89: Electron backscatter image of sample 12 showing large fractures perpendicular and parallel to the edge of the sample. Smaller fractures occur perpendicular to the edge of the sample.

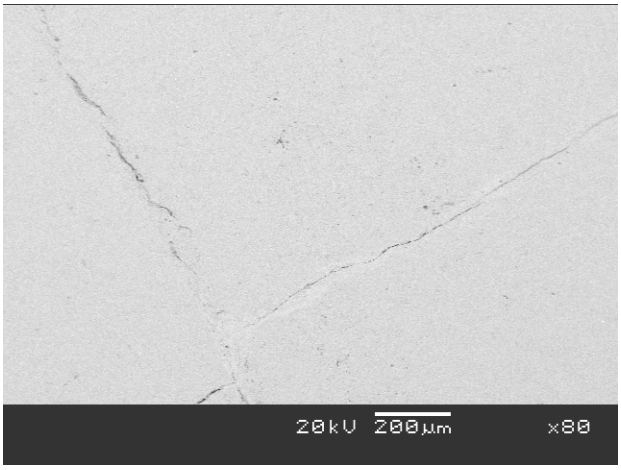

Figure 90: Electron backscatter image of sample 17 showing regularly spaced fracture/joint set in the sample.

3.4.2 GROUP 2: POLY-MINERALIC SAMPLES

This group of samples have a significant proportion of gangue minerals. The results from the various samples in this group indicates that the presence of gangue minerals alone do not cause fractures to form. However, the gangue minerals do influence the direction and intensity of fractures and gangue minerals. Especially quartz, that is much harder than hematite tend to fracture more easily than hematite.

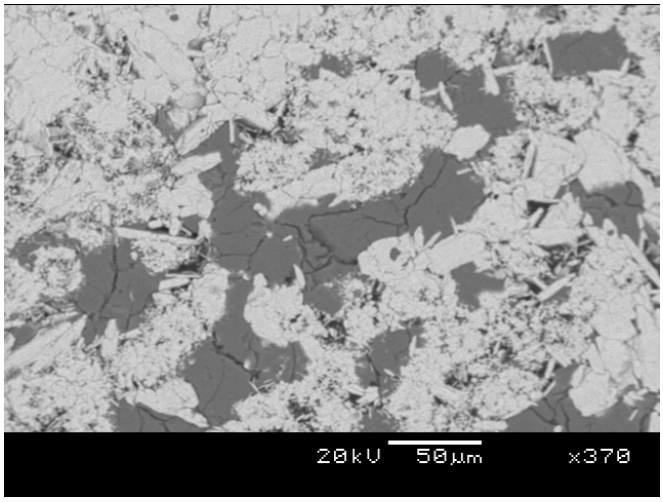

Figure 91: Electron backscatter image of sample 1 showing fractures originating and terminating within quartz (grey) without extending into the surrounding hematite.

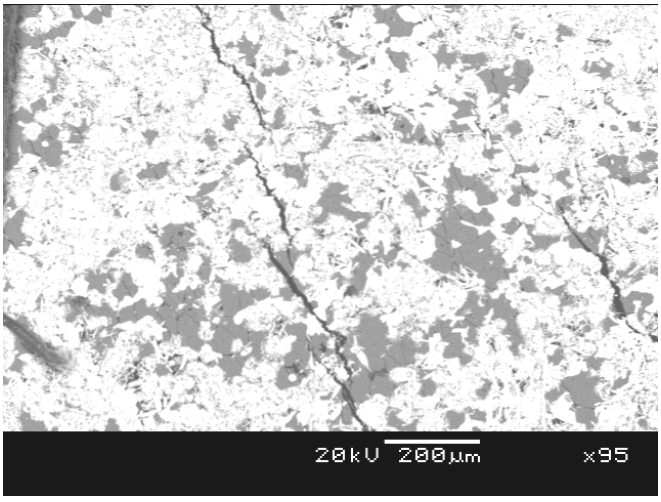

Figure 92: Electron backscatter image of sample 1 showing large fractures that do not appear to be influenced by the sample mineralogy. The fractures propagate through both gangue and ore minerals.

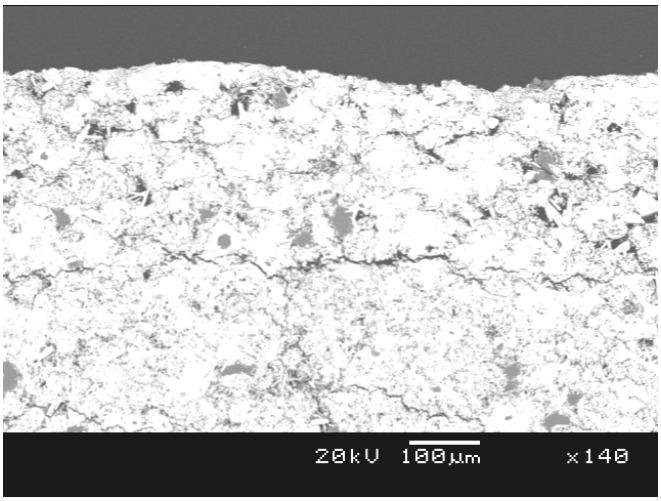

Figure 93: Electron backscatter image of sample 1 showing regularly spaced fractures at the edge of the sample, related to the volume change during the reduction of hematite to magnetite.

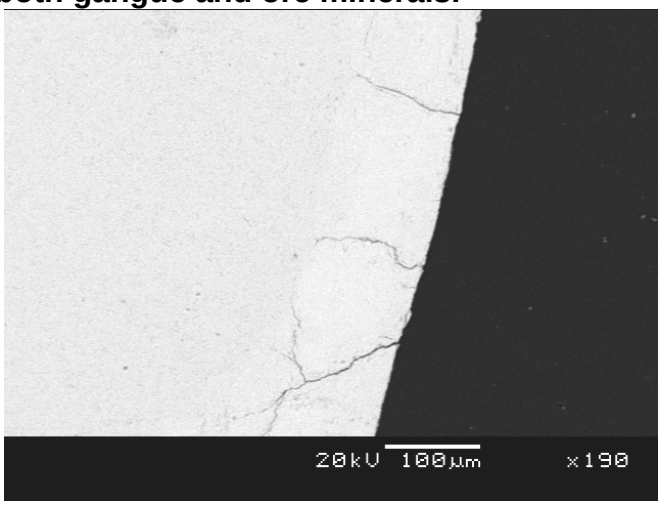

Figure 94: Electron backscatter image of sample 10 showing the development of fractures along the edge of the samples, where it has been reduced. The stippled line indicates where the sample has been reduced.

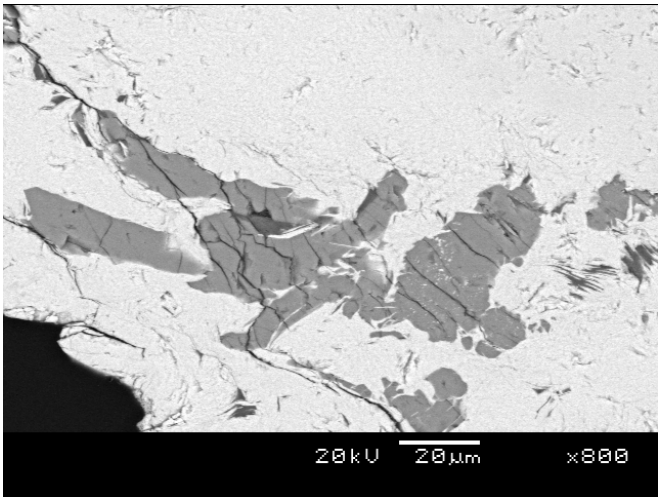

Figure 95: Electron backscatter image of sample 10 showing the development of fractures in quartz. The secondary fractures do not extend into the surrounding hematite.

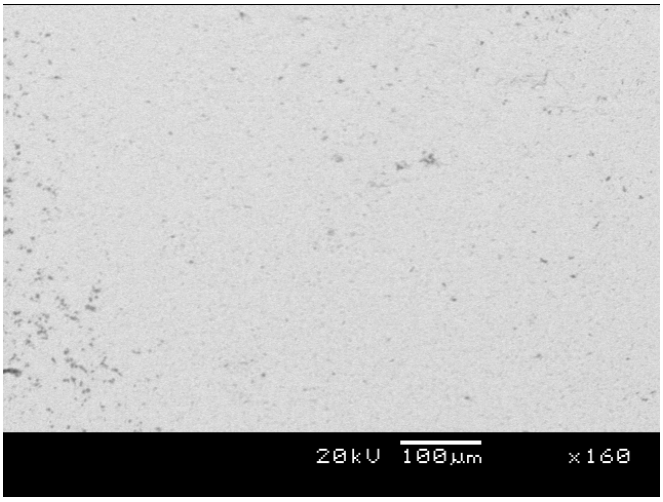

Figure 96: Electron backscatter image of sample 10 showing an area within the sample where no reduction or fracturing has occurred.

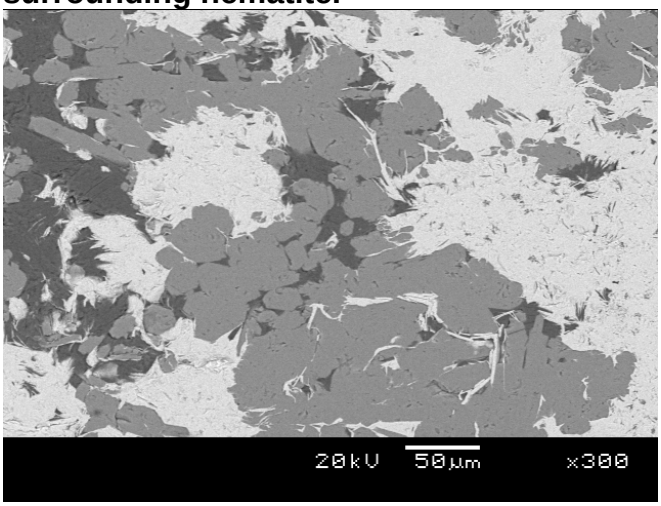

Figure 97: Electron backscatter image of sample 10 showing intergrown hematite and gangue. The presence of gangue phases does not necessarily lead to fracture formation.

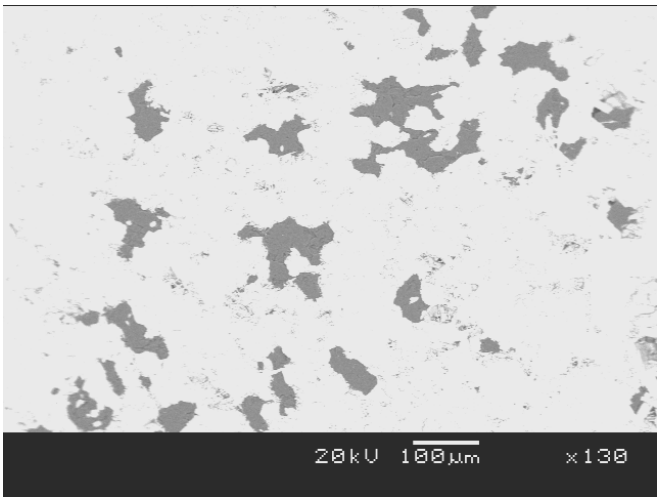

Figure 98: Electron backscatter image of sample 14 showing intergrown hematite and quartz in the center of the sample. There are o fractures observed here as no reduction has been able to occur with the low sample porosity.

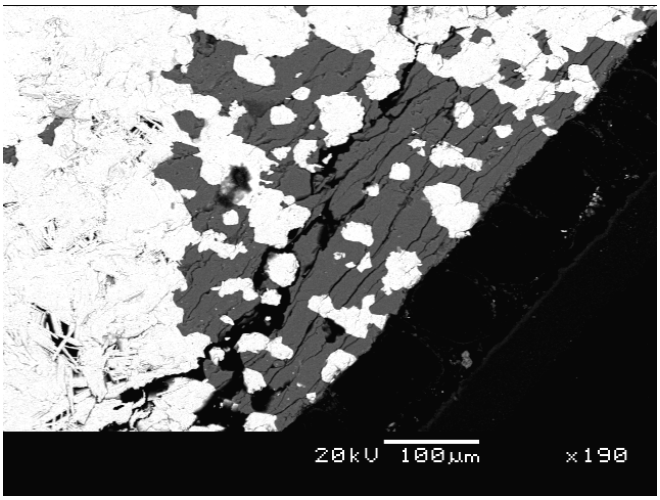

Figure 99: Electron backscatter image of sample 14 showing fractures developed at the edge of the sample where reduction has occurred. Notice how the gangue allows for more extensive development of the fracture network that does not extend into the surrounding hematite.

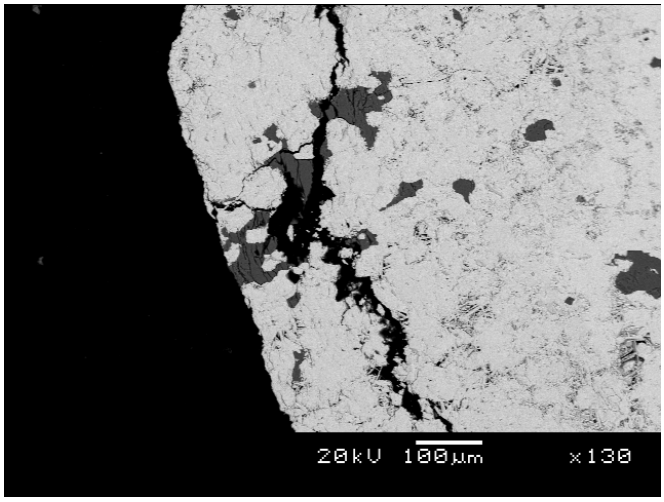

Figure 100: Electron backscatter image of sample 14 showing fractures developed along the edge of the sample where it has been reduced. Where a fracture intersects gangue minerals the gangue appears to facilitate the development of fractures.

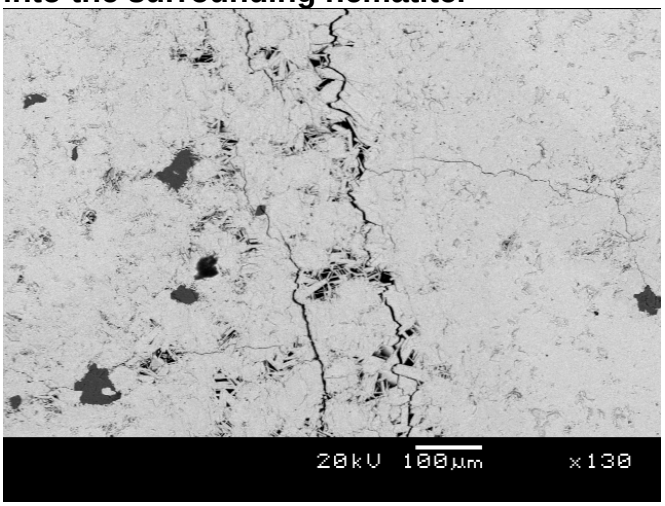

Figure 101: Electron backscatter image of sample 14 showing fractures developed within the sample. The fractures appear to join open pores where reduction has occurred.

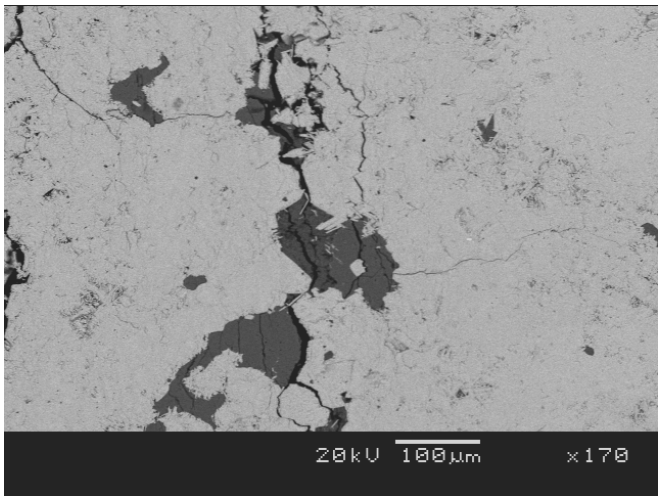

Figure 102: Electron backscatter image of sample 14 showing fractures developed within the sample. Where a fracture intersects gangue minerals the gangue appears to facilitate the development of fractures that do not extend into the surrounding hematite.

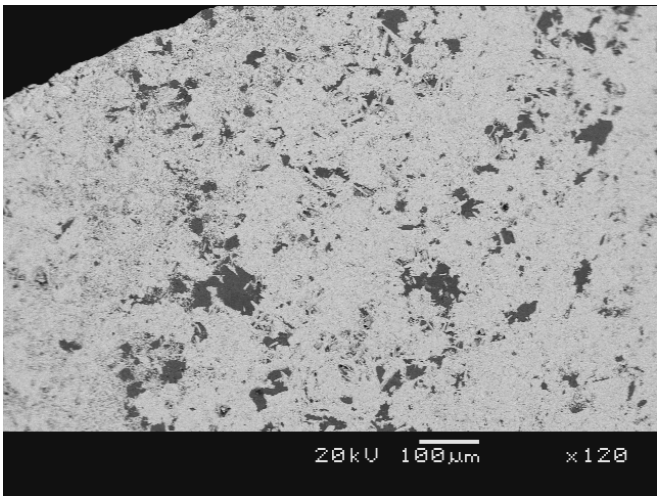

Figure 103: Electron backscatter image of sample 15 showing intergrown hematite and gangue with very low porosity and no visible fractures, even at the edge of the sample where fractures are unusually prolific.

3.4.3 GROUP 3: POROUS SAMPLES

Only two porous samples were identified in the study. Sample 2 consists of bands of acicular hematite with very high porosity whilst sample 16 has a homogenous high-porosity texture throughout the sample. Neither sample exhibits extensive fracturing. One could argue that the numerous open voids present in the samples could possibly accommodate for the volume change that takes place during reduction and thus less fracturing is observed in these samples.

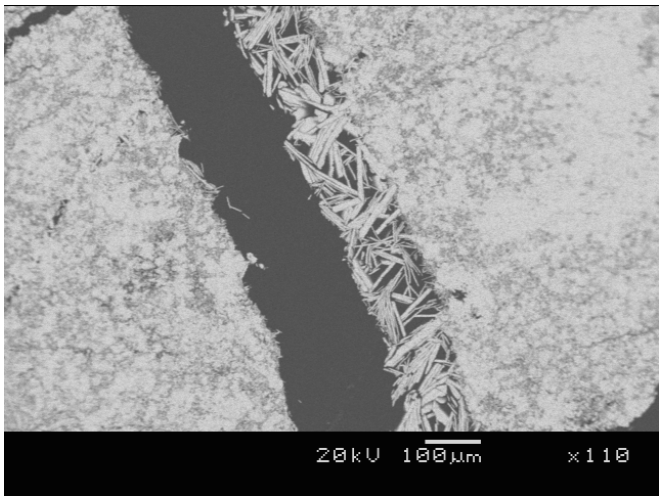

Figure 104: Electron backscatter image of sample 2 showing a very large fracture that has occurred at a boundary between granular hematite (left) and porous specularite (acicular hematite).

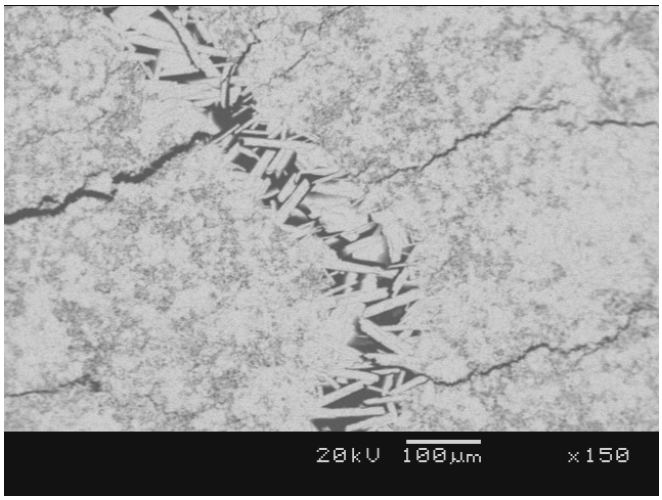

Figure 105: Electron backscatter image of sample 2 showing large fractures originating/terminating in areas of low porosity.

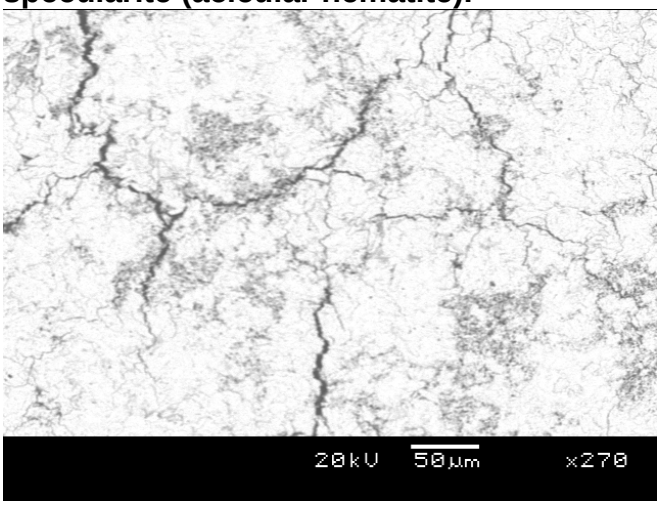

Figure 106: Electron backscatter image of sample 2 showing a network or regularly spaced and oriented fractures formed in an area of dense homogenous ore.

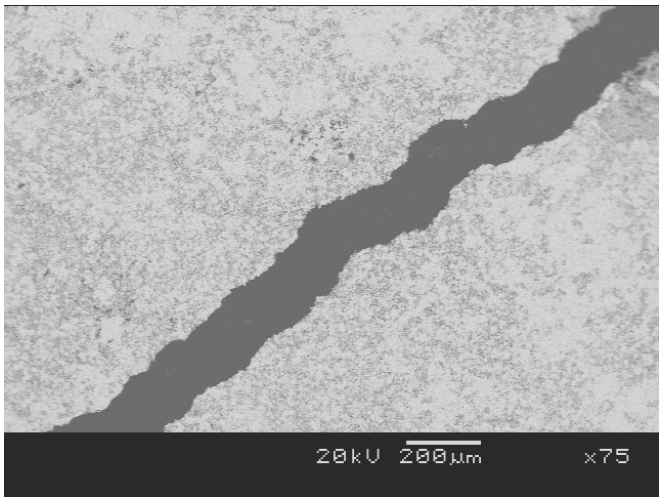

Figure 107: Electron backscatter image of sample 2 showing a large fracture through low porosity granular hematite. The fracture occurs without a large network of feeder fractures or ancillary fractures.

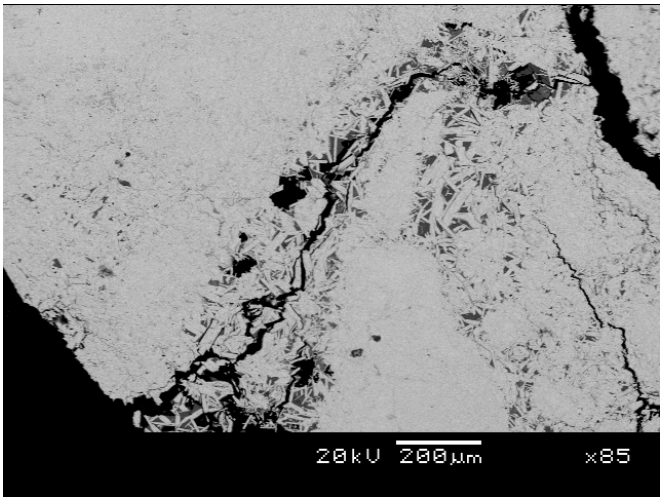

Figure 108: Electron backscatter image of sample 16 showing a large fracture associated with acicular hematite.

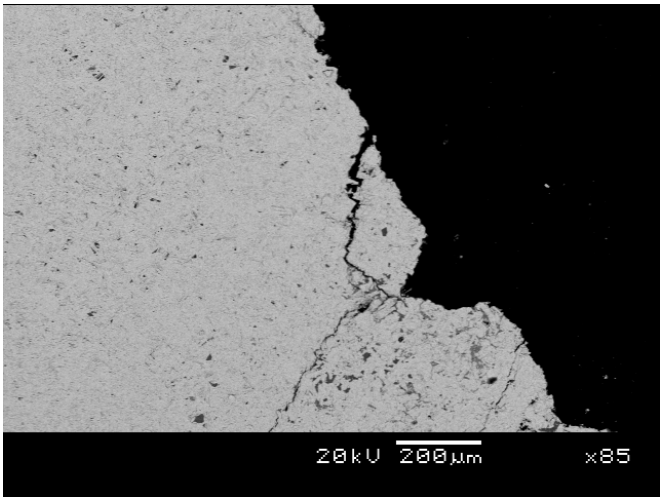

Figure 109: Electron backscatter image of sample 16 showing a small fracture at the edge of the sample associated with reduction of hematite.

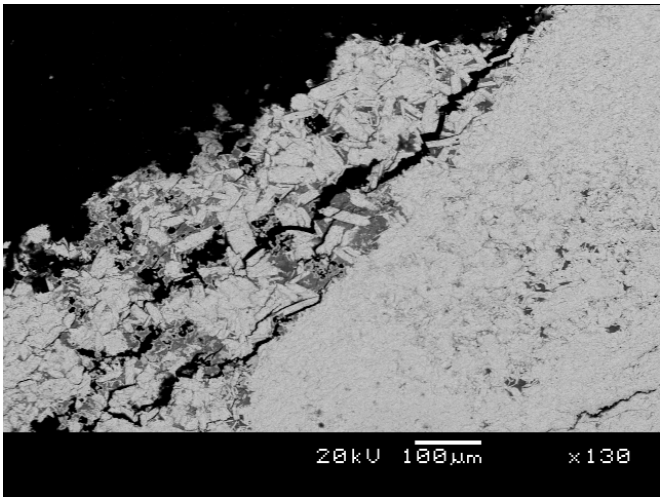

Figure 110: Electron backscatter image of sample 16 showing fractures at the edge of the sample where reduction has taken place. The influence of acicular hematite and gangue minerals is uncertain.

3.4.4 GROUP 4: OTHER

Only in one sample, Sample 6, could the fracture patterns not be linked to any compositional or textural features in the sample. Fractures were orientated parallel to the foliation fabric or in a regularly spaced network of fractures that occurred at right angles to each other.

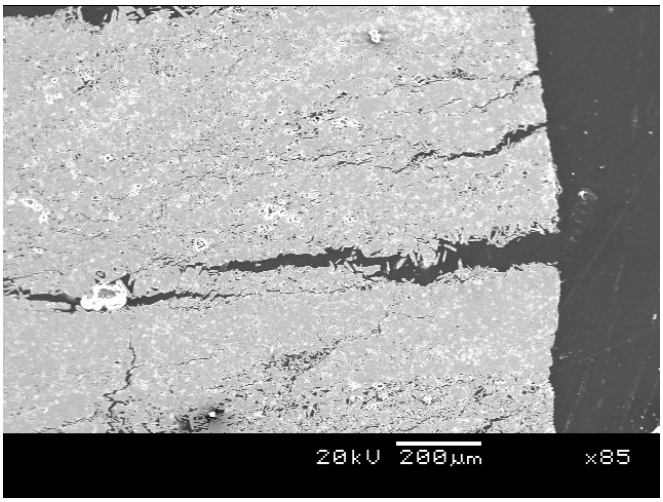

Figure 111: Electron backscatter image of sample 6 showing fractures oriented parallel to the foliation fabric.

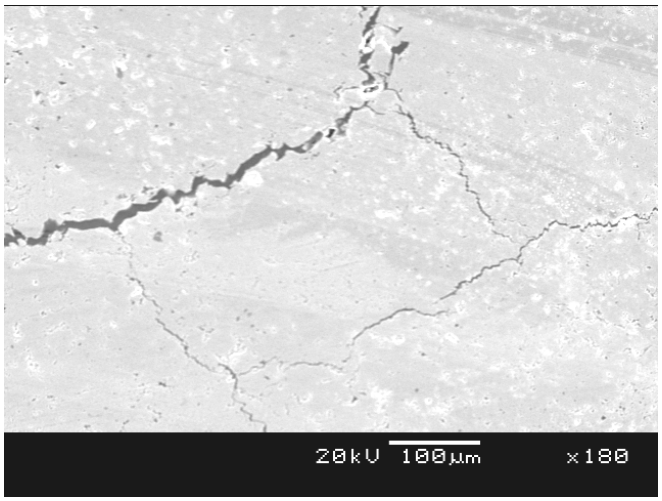

Figure 112: Electron backscatter image of sample 6 showing a regularly spaced network of fractures that occur at right angles to each other. There are no compositional or textural features to influence the fracture orientation.